Technical Report Documentation Page

1. Report No.	2. Government Accession No.	3. Recipient's Catalog No.
FHWA/TX-91+1123-7F		

4. Title and Subtitle	5. Report Date
THE FALLING WEIGHT DEFLECTOMETER AND SPECTRAL ANALYSIS OF SURFACE WAVES TEST FOR CHARACTERIZING PAVEMENT MODULI: A CASE STUDY	February 1991
	6. Performing Organization Code
7. Author(s) K. H. Stokoe, II, W. R. Hudson, and B. F. Miner	8. Performing Organization Report No. Research Report 1123-7F
9. Performing Organization Name and Address Center for Transportation Research The University of Texas at Texas at Austin Austin, Texas 78712-1075	10. Work Unit No. (TRAIS) 11. Contract or Grant No. Rsch. Study 2/3-18-87/9-1123
12. Sponsoring Agency Name and Address Texas Department of Transportation (formerly State Department of Highways and Public Transportation) P. O. Box 5051 Austin, Texas 78763-5051	13. Type of Report and Period Covered Final 14. Sponsoring Agency Code

15. Supplementary Notes

Study conducted in cooperation with the U. S. Department of Transportation, Federal Highway Administration. Research Study Title: "Non-Destructive Test Procedures for Analyzing the Structural Conditions of Pavements"

16. Abstract

This report details the results of tests on newly constructed flexible pavement using a Dynatest 9000 Falling Weight Deflectometer and the Spectral Analysis of Surface Waves test. Additional types of field and laboratory tests were also undertaken and are reported in this study. Taken together, the data and analyses represent a detailed case study of the two non-destructive test methods.

When dynamic effects and the demonstrated non-linear behavior of the soil are accounted for, Spectral Analysis of Surface Waves and the Falling Weight Deflectometer provide similar subgrade moduli. The excitation frequency of Spectral Analysis of Surface Waves and the Falling Weight Deflectometer differ by two to three orders of magnitude in the surface layer, and one to two orders of magnitude in the subgrade. However, results from Spectral Analysis of Surface Waves and Falling Weight Deflectometer tests for the asphalt concrete are consistent when adjusted to a common frequency.

Spectral Analysis of Surface Waves and the Falling Weight Deflectometer were both useful for characterizing the material of Ramp SW. Analysis and application of the data from these techniques should include consideration of dynamic loading, non-linear behavior in the subgrade, and frequency sensitivity in the asphalt.

17. Key Words	18. Distribution Statement
pavement evaluation, Young's modulus, Falling Weight Deflectometer (FWD), seismic waves, Spectral Analysis of Surface Waves (SASW)	No restrictions. This document is available to the public through the National Technical Information Service, Springfield, Virginia 22161.

19. Security Classif. (of this report)	20. Security Classif. (of this page)	21. No. of Pages	22. Price
Unclassified	Unclassified	52	

THE FALLING WEIGHT DEFLECTOMETER AND SPECTRAL ANALYSIS OF SURFACE WAVES TEST FOR CHARACTERIZING PAVEMENT MODULI: A CASE STUDY

by

K. H. Stokoe, II
W. R. Hudson
B. F. Miner

Research Report Number 1123-7F

Research Project 2/3-18-87/9-1123

Non-Destructive Test Procedures for Analyzing the Structural Conditions of Pavements

conducted for

Texas State Department of Highways and Public Transportation

in cooperation with the

**U. S. Department of Transportation
Federal Highway Administration**

by the

CENTER FOR TRANSPORTATION RESEARCH

Bureau of Engineering Research

THE UNIVERSITY OF TEXAS AT AUSTIN

February 1991

NOT INTENDED FOR CONSTRUCTION, PERMIT, OR BIDDING PURPOSES

K. H. Stokoe, II, P.E. (Texas No. 49095)
W. R. Hudson, P.E. (Texas No. 16821)
Research Supervisors

PREFACE

This report—the final for Research Project 1123—summarizes results from a case study involving the Falling Weight Deflectometer and the Spectral Analysis of Surface Waves test. These two methods were used to characterize the moduli of pavement layers.

Research was conducted through the Center for Transportation Research, The University of Texas at Austin, and was sponsored by the Texas State Department of Highways and Public Transportation.

The authors wish to acknowledge the valuable assistance provided by the staff of the Center for Transportation Research. We particularly would like to cite the contributions of Dr. Jose Roesset, Dr. German Claros, Mr. Der-Wen Chang, Mr. James Bay, Mr. Marwan Aouad, Mr. Ron Andrus, Mr. Hassan Torshizi, and Mr. Dong-Soo Kim. In addition, we would like to thank the staff of the State Department of Highways and Public Transportation for generously providing both test equipment and access to a convenient test site.

K. H. Stokoe, II
W. R. Hudson
R. F. Miner

LIST OF REPORTS

In addition to six other reports—Research Reports 1123-1, -2, -3, and -4F, submitted by the Texas Transportation Institute of Texas A&M University, and Research Reports 1123-5 and -6, submitted by the Center for Transportation Research of The University of Texas at Austin—documentation for this research project includes the following.

Research Report Number 1123-7F, "The Falling Weight Deflectometer and Spectral Analysis of Surface Waves Test for Characterizing Pavement Moduli: A Case Study," by K. H. Stokoe, II, W. R. Hudson, and R. F. Miner, presents the results of tests on newly constructed flexible pavement using the Falling Weight Deflectometer and the Spectral Analysis of Surface Waves method. The dynamic effects, the non-linear behavior in the subgrade, and the frequency sensitivity in the asphalt were aspects of these tests that received particular consideration. February 1991.

ABSTRACT

This report details the results of tests on newly constructed flexible pavement using a Dynatest 9000 Falling Weight Deflectometer and the Spectral Analysis of Surface Waves test. Additional types of field and laboratory tests were also undertaken and are reported in this study. Taken together, the data and analyses represent a detailed case study of the two non-destructive test methods.

When dynamic effects and the demonstrated non-linear behavior of the soil are accounted for, Spectral Analysis of Surface Waves and the Falling Weight Deflectometer provide similar subgrade moduli. The excitation frequency of Spectral Analysis of Surface Waves and the Falling Weight Deflectometer differ by two to three orders of magnitude in the surface layer, and one to two orders of magnitude in the subgrade. However, results from Spectral Analysis of Surface Waves and Falling Weight Deflectometer tests for the asphalt concrete are consistent when adjusted to a common frequency.

Spectral Analysis of Surface Waves and the Falling Weight Deflectometer were both useful for characterizing the material of Ramp SW. Analysis and application of the data from these techniques should include consideration of dynamic loading, non-linear behavior in the subgrade, and frequency sensitivity in the asphalt.

KEY WORDS: pavement evaluation, Young's modulus, Falling Weight Deflectometer (FWD), seismic waves, Spectral Analysis of Surface Waves (SASW)

SUMMARY

A newly constructed highway overpass embankment in Austin, Texas, was extensively tested using both a Dynatest 9000 Falling Weight Deflectometer (FWD) and the Spectral Analysis of Surface Waves (SASW) method; other types of field and laboratory tests were performed as well. Taken together, the data and analyses represent a detailed case study and comparison of the two non-destructive test methods (including their ability to determine pavement stiffness properties).

Conventional static back-calculation for the FWD does not model the dynamic aspects of the FWD. And SASW measures the subgrade modulus at small strains. When dynamic effects and the demonstrated non-linear behavior of the soil are accounted for, SASW and the FWD provide similar subgrade moduli.

The excitation frequency of SASW and the FWD differ by approximately two to three orders of magnitude. The modulus of asphalt concrete is sensitive to testing frequency, and SASW and FWD results for the asphalt concrete are consistent when adjusted to a common frequency.

SASW and the FWD were both useful for characterizing the material of Ramp SW. Analysis and application of the data from these techniques should include consideration of the dynamic loading, the non-linear behavior in the subgrade, and the frequency sensitivity in the asphalt.

IMPLEMENTATION STATEMENT

Pavement evaluation using the Falling Weight Deflectometer (FWD) and the Spectral Analysis of Surface Waves test (SASW) is common in pavement research at both The University of Texas at Austin and the Texas State Department of Highways and Public Transportation. Because these evaluation methods of analysis for both methods and SASW field equipment and techniques are still subjects of promising ongoing development, the data contained in this report should be useful as a basis for testing further developments. Specifically, the relatively comprehensive case study represented by this report can assist research into non-linear and dynamic analysis of FWD data. Also, the role of SASW testing and the relevance of SASW results are presented in a manner that supports both research and practical applications. Thus, the conclusions and recommendations contained in this report suggest areas for future research while, at the same time, providing guidance for routine testing.

TABLE OF CONTENTS

CHAPTER 1. INTRODUCTION

Non-destructive evaluations (NDE) of pavement structures provide several benefits not offered by laboratory tests of sampled material. For example, such evaluations conducted in situ automatically provide realistic conditions of stress, strain, temperature, and moisture. Moreover, an NDE test conducted with rapid and simple procedures can provide—for relatively low cost—many individual measurements of material properties. Thus, a reliable and efficient NDE method allows economical measurement of the realistic values and the variations of material properties in a pavement section.

These advantages distinguish NDE from laboratory testing in several ways. First, laboratory evaluation of material properties requires that one obtain, transport, store, prepare, and test the samples under conditions that—it is hoped—model those in the field. Second, solutions to specific sampling and testing problems are often expensive. Finally, individual tests may not represent average in-situ material properties.

This report, sponsored by the Texas State Department of Highways and Public Transportation (SDHPT), focuses on two NDE methods: the Falling Weight Deflectometer (FWD) and the Spectral-Analysis-of-Surface-Waves (SASW). While both of these techniques are subjects of past and current research, this report uses specific data obtained from a case study to evaluate and compare the sensitivity and performance of FWD and SASW.

The study was conducted on overpass Embankment SW of the interchange between US Loop 1 and US 183 in Austin, Texas. This embankment was constructed with select rock fill placed over natural soil and limestone bedrock, with the width and length of the embankment measuring approximately 50 and 350 feet, respectively. As shown in Fig 1.1, fill thickness increases as the elevation of the embankment's surface increases. The pavement profile (Fig 1.2) consists of limestone bedrock, several feet of natural soil, a compacted fill of varying thicknesses, 6 inches of crushed limestone base, and 7 inches of asphalt concrete. The variation of soil thickness between the sloped highway surface and the nearly horizontal rock stratum is a key feature of the site.

The fill for Embankment SW was placed between December 1988 and February 1989, with a crushed limestone base laid in March 1989. Four inches of Type-A asphalt concrete was placed during late May, and a 3-inch course of Type-C asphalt concrete was added during early June 1989. Placement of a final 1.5-inch surface course

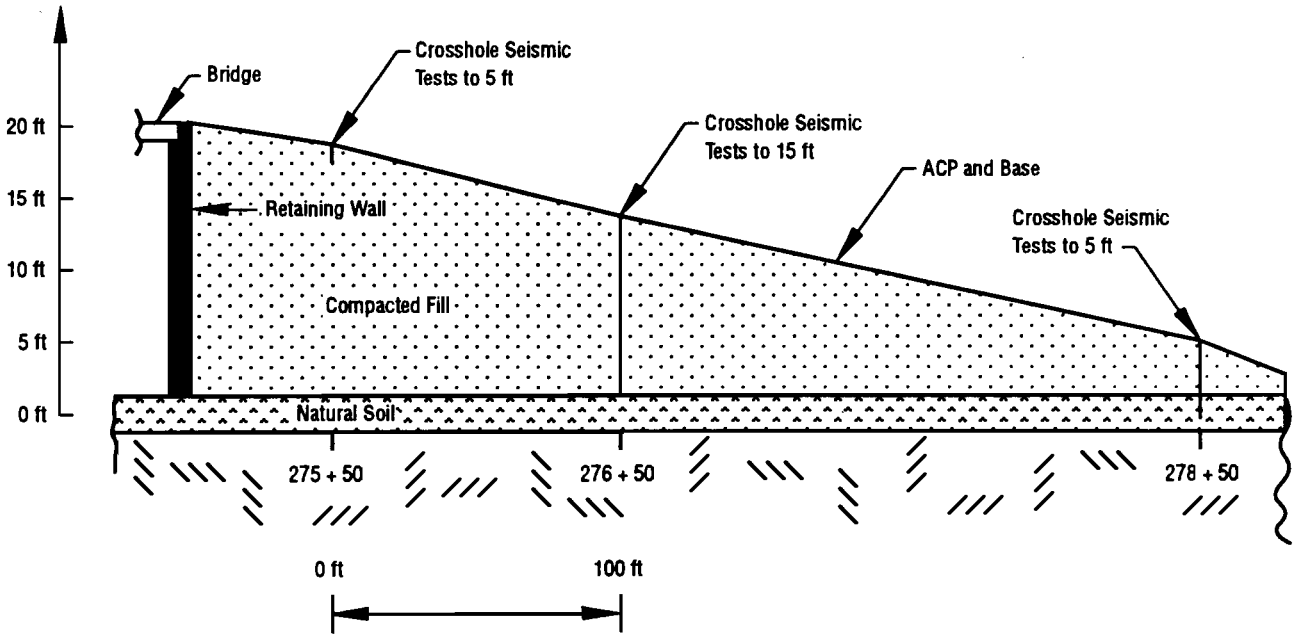

Fig 1.1. Approximate longitudinal cross-section of Embankment SW.

will occur after Embankment SW enters service. Core samples of the asphalt concrete indicated that their thicknesses were close to the design values shown in Fig 1.2.

Initial site investigation, which began after placement of the crushed limestone base, consisted of crosshole seismic tests conducted in boreholes near upper, middle, and lower locations on Embankment SW. Five 3-inch-diameter sample tubes were pushed in boreholes drilled for the crosshole tests.

Samples from the pushed tubes provided material for resilient modulus and resonant column tests. When the profile shown in Fig 1.2 was complete, 2-inch- and 4-inch-diameter samples of the asphalt concrete were cored and then subjected to resilient modulus and resonant column tests in laboratories at The University of Texas.

SASW tests were conducted over the crushed limestone base before placement of any asphalt concrete. With the 4-inch layer of asphalt in place, both FWD and additional SASW tests were conducted; these tests were then repeated once the asphalt reached its total thickness of 7 inches. Tests over the asphalt were made at 50-foot intervals within a 350-foot section of Embankment SW (Stations 275+50 to 278+50). Finally, daily temperatures within the asphalt concrete were carefully monitored with thermocouples, and tests were conducted under minimum and maximum asphalt temperatures.

The overall testing program yielded a set of FWD and SASW test data within which the depth to rock, asphalt temperature, and asphalt thickness varied independently. This data set, together with supplemental data from other types of tests, provided the basis for the present case study. In addition to presenting final results and conclusions, subsequent chapters in this report detail specific field and analytical procedures.

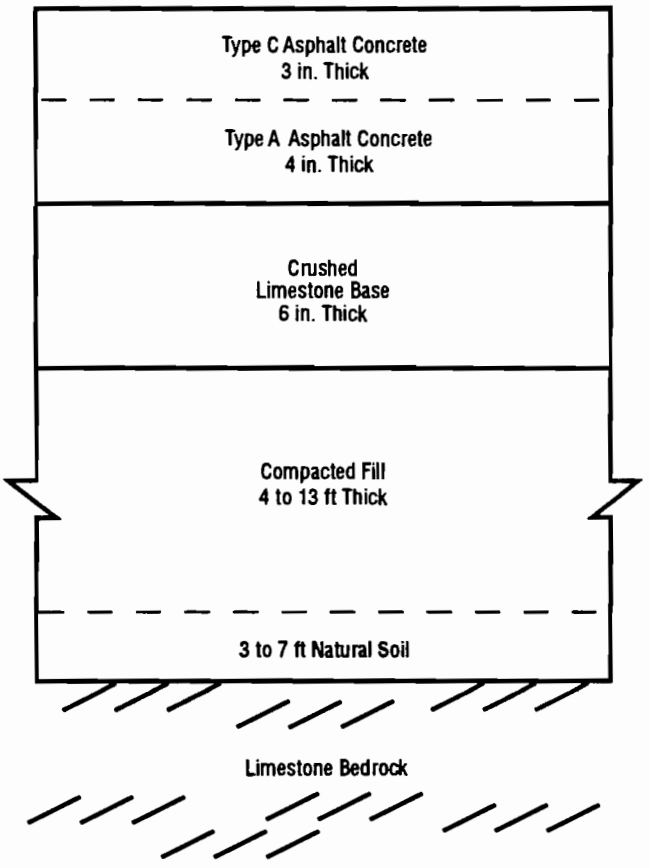

Fig 1.2. Simplified profile of Embankment SW, Austin, Texas.

CHAPTER 2. THE FALLING WEIGHT DEFLECTOMETER

GENERAL DESCRIPTION

A Falling Weight Deflectometer (FWD) is a trailer-mounted apparatus capable of (1) generating an impulsive load and (2) measuring resulting pavement deflections. Figure 2.1 below shows the basic layout of a Dynatest FWD Model 9000—the SDHPT-owned FWD used to collect data in this study.

The FWD's impulsive load is generated by dropping a rigid set of steel weights on rubber cushions which rest on a steel loading plate. The rigid circular loading plate has a 5.91-inch radius and is separated from the pavement surface by a thin rubber pad. Peak loads were varied by changing the drop height, with the same total weight used for all tests. In standard practice, peak loads are controlled by the total weight, the drop height, and the impedance (or stiffness) of a pavement profile. For common pavement profiles the range of possible peak impact loads is approximately 2 to 25 kips. Net effective contact pressures for such loads are between 18 and 245 psi.

Dynatest literature for the Model 9000 FWD claims that the peak load was measured with an accuracy of 2 percent ±280 lbs; thus, for a 9,000-lb load the expected maximum error was 5 percent. Bentson, Nazarian, and Harrison (Ref 1) reported an independent comparison of a Dynatest FWD's internal load measurement with load cells placed under the loading pad. They found approximately 4.3 percent error at a 7.8-kip load and 3.0 percent error at a 25-kip load. Based on these data, it seems reasonable to expect the FWD to provide a load measurement accuracy of about 4 percent for typical operations.

The function of the loading system is to provide a series of distinct impulses during each drop. Figure 2.2 is a plot of velocity versus time recorded with a vertical velocity transducer (geophone) placed 4.5 inches below the surface and directly under the load center. This transducer was placed in the Flexbase before the 4-inch layer of asphalt concrete was applied. The first peak in Fig 2.2 has the highest velocity, which is due to the weight falling from the nominal drop height. Subsequent impulses are associated with "bounces" of the loading system. A Fourier series power spectrum of a similar velocity record is shown in Fig 2.3. Most of the impact energy is transmitted between frequencies of 2 and 40 Hz.

Data acquisition in the Dynatest FWD was triggered by a proximity switch whose voltage changed just before impact. Following this trigger, the FWD collected data for 60 milliseconds—a period providing a record of the load and displacements associated with the first and largest impulse. Figure 2.4 shows a time history of the load and displacements recorded by the FWD during testing on Embankment SW with 7 inches of asphalt concrete. The curve labeled "LOAD" shows the magnitude of transient force immediately above the loading plate as measured with the FWD instrumentation. For this impact, the load reached a peak approximately 12 milliseconds after impact, with the total duration of significant loading lasting approximately 30 milliseconds.

Deflection data are obtained from a line of geophones, the position and spacing between which is varied manually by the FWD operator. During tests conducted for this report, the standard SDHPT geophone

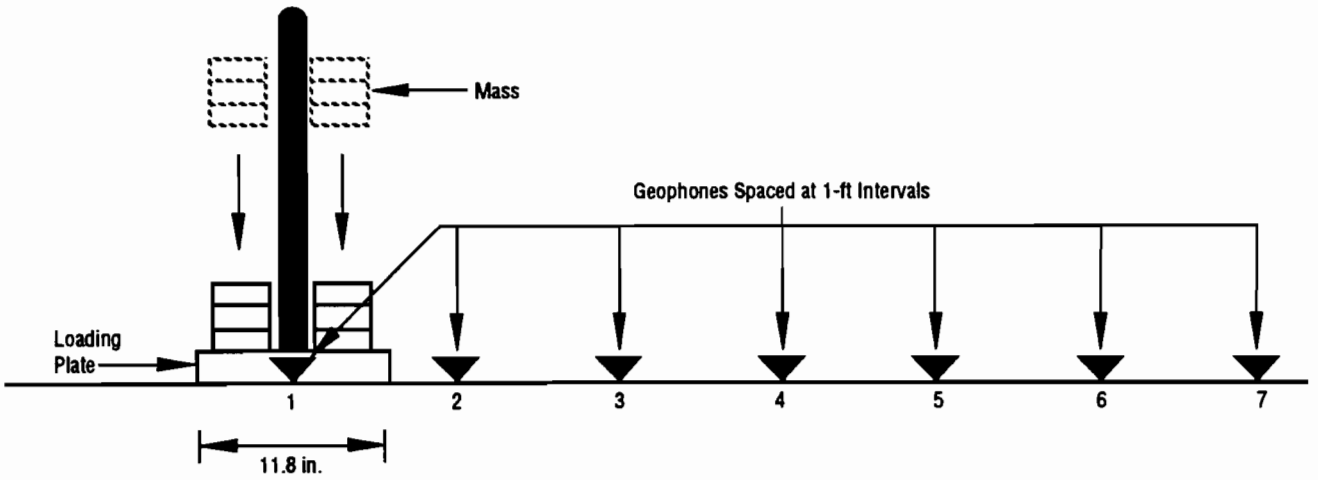

Fig 2.1. Layout of the Dynatest 9000 Falling Weight Deflectometer with seven geophones in the standard SDHPT configuration.

configuration was used. In this configuration seven geophones were spaced at 1-foot intervals, with the first geophone at the center of the loading pad. The Dynatest data acquisition equipment integrated the measured velocity to obtain the deflection. Time histories of deflection at all geophone locations are shown in Fig 2.4, together with the load history. Numerical data for these histories were obtained from the FWD using options in the Dynatest software.

Dynatest performance specifications for deflection measurement with the Dynatest 9000 FWD claim an absolute accuracy of 2 percent ±0.08 mils, and a resolution of 0.4 mils (1 mil equals 0.001 inch). Independent investigation of the accuracy and repeatability of FWD measurements suggested that deflections were typically measured with an accuracy of between 2 and 8 percent (Ref 1). However, absolute deflections are inversely related to distance from the load plate; thus, typical percentage variation measurements increase with distance from the load center.

Peak deflections and peak force are routinely used to define the load-deflection relation (basin) for a pavement. During normal operation, the Dynatest system stores and prints only these peak values. The resulting load and "basin" are a simplification, because the load is dynamic and the peaks of individual deflections are not necessarily simultaneous. However, in Fig 2.4, the peaks usually occur quite closely in time, particularly for locations close to the load. Thus, the deepest "instantaneous" basin may be quite similar to the "basin" defined by non-simultaneous peak deflections.

METHODS OF ANALYSIS

Methods of analyzing FWD deflection data appear to fall into two categories or approaches. One approach utilizes differences and/or ratios between deflections

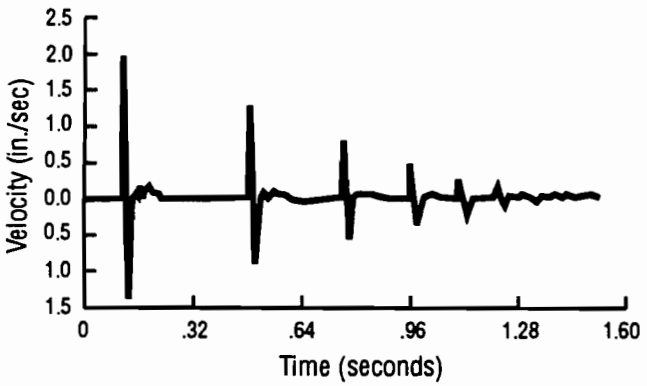

(a) Full time history showing multiple impulses of FWD.

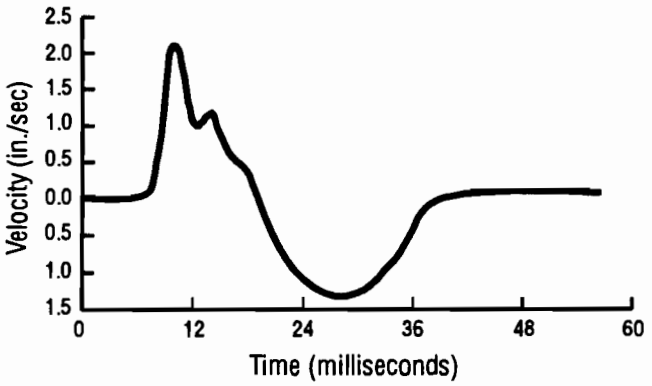

(b) Primary impact with expanded time scale.

Fig 2.2. Time history of velocity due to an FWD impact, measured at a depth of 4.5 inches below the surface of a 4-inch-thick asphalt pavement (Embankment SW Station 276+50).

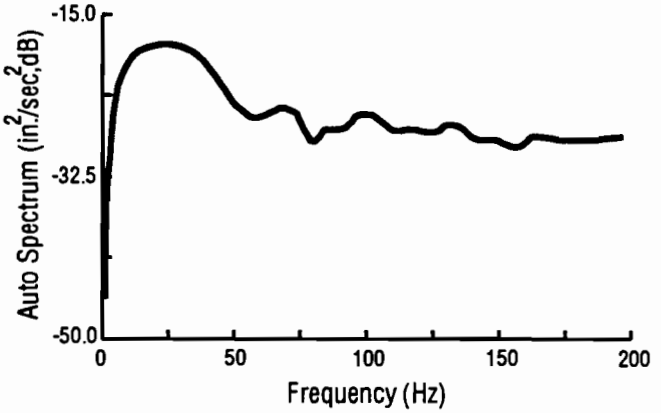

(a) Decibel scale.

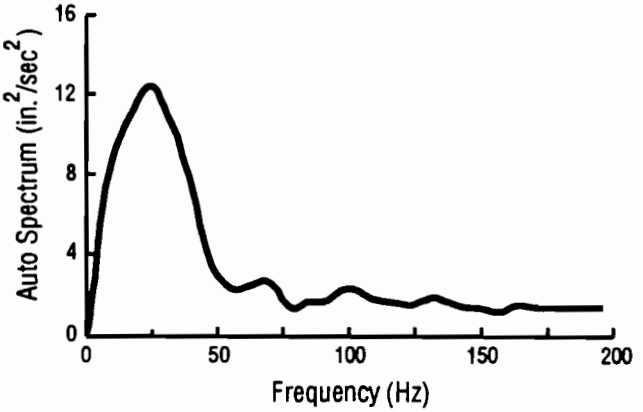

(b) Linear scale.

Fig 2.3. Auto spectrum of velocity due to an FWD impact, measured at a depth of 8 inches, with 7 inches of asphalt concrete.

measured at different locations during a single test. This method is the most common form of analysis for load transfer across joints and for empirical indices of pavement performance (Ref 2). Because the work reported herein is focused on characterization of material properties, these ratios and indices are not discussed.

The second approach is often referred to as "basin fitting." Hypothetical moduli of a layered system are adjusted until a computed deflection basin matches the measured deflection basin. If the basins match well, the moduli used for the computed basin are taken as a good representation of moduli in situ. This approach is thus an iterative one and may utilize a static or a dynamic model to compute deflections for the hypothetical system and load. Static basin-fitting algorithms are generally coupled with such computer programs as ELSYM5, CHEVRON, or BISAR (Refs 3 and 4), all of which perform a static analysis of a system with linearly elastic layers and yield a computed static deflection basin. These static analysis programs follow the assumptions of Burmister (Ref 3). (A useful summary of these assumptions and the features of prominent programs have been compiled by Hicks; see Ref 4.) A methodology and algorithm using such programs for fitting deflection basins was presented by Uddin working under Project 387 of the Center for Transportation Research at The University of Texas at Austin (Ref 5). The computer programs FPEDD and RPEDD were developed as part of Uddin's work. Both of these programs utilize the ELSYM5 layer analysis program within a self-iterative basin-matching algorithm.

These and other similar basin-matching programs such as BISDEV and CHEDEF (Ref 6) require user input of a thickness, a Poisson's ratio, and an estimated Young's modulus for each layer. Deflection basins that were computed using the estimated or initial default moduli are compared against a measured basin. The error between measured and computed basins is used to estimate new trial moduli; deflections are then recomputed.

This automatic iterative procedure continues until the basin match error is less than some tolerance or until a given maximum number of different computed basins have been tried. The combination of moduli which give the smallest error function between computed and measured basins is considered to represent the pavement layers. The error function is based on the sum of the squares of the differences between computed and measured deflection for specific radial distances.

For each basin subjected to backcalculation, the basin-matching procedure described above requires numerous iterations of a multi-layer program. An improvement to this approach has been reported by Uzan of the Texas Transportation Institute (Ref 7) and coded in the MODULUS program for microcomputers. The basin-fitting approach utilized in MODULUS involves computation and storage of deflection basins for a matrix of modular ratios representing up to four layers of known thicknesses. Once this data bank is established using an appropriate multi-layer program, a search routine is invoked to minimize the error between measured basins and basins in the data bank (or basins interpolated from the data bank). For this report, most static analyses of FWD data were made with MODULUS.

Dynamic analysis of layered systems, less common than static analysis, is the subject of study in Center for Transportation Research (CTR) Project 1123. Roesset and Shao discussed the importance of dynamic analysis for steady-state equipment such as the Dynaflect and for transient loads such as those from an FWD (Ref 8). Large dynamic amplifications were shown for soil systems loaded at a frequency close to their fundamental frequency. Anderson and Drenvich (Ref 9) published a case study involving dynamic and static analysis of tests with a Road Rater (steady-state harmonic excitation) on a rigid pavement with 133 feet until bedrock. In their study, the results of static and dynamic analyses were significantly different from each other. Static analyses appeared to underpredict the modulus of the portland cement concrete surface layer and overpredict the modulus of the subgrade.

The UT computer program used for dynamic analysis of FWD data in the present study is a modification of the program described by Roesset and Shao (Ref 8). This analysis is a descretized Green's solution and utilizes the theory of wave propagation in a system of infinitely wide linear elastic layers. The global stiffness matrix formulation presented by Kausel and Roesset (Ref 10) provides an explicit solution for the deflections resulting from a harmonic load at a single frequency. The current UTPV program implements a routine to compute automatically an appropriate mesh for a descretized Green's solution of

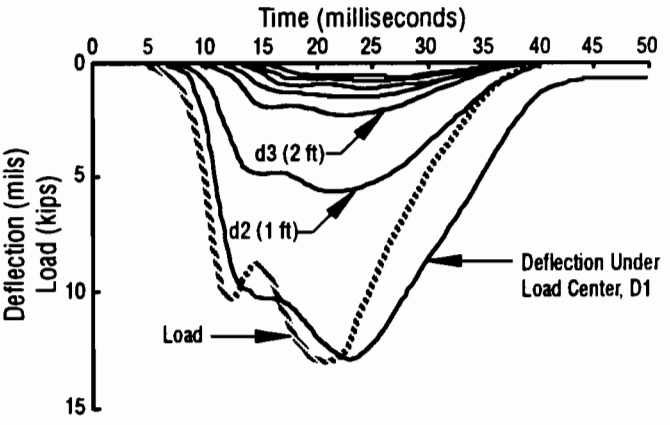

Fig 2.4. Time history of load and deflections as recorded by a Dynaflect 9000 FWD on 7 inches of asphalt concrete, ramp SW, June 3, 1989.

each frequency. Analyses of a suitable number of frequencies within the range of relevant frequencies yield an approximate transfer function for all points on the surface where deflection is computed. Each transfer function is then multiplied by the Fourier Transform of the transient FWD load-pulse to obtain the frequency domain response at each point. Finally, the time history of motion at each point is given by the inverse Fourier Transform of the computed frequency domain response.

Peak deflections for each geophone location were the desired output from a dynamic analysis. These peaks were obtained directly from the computed time histories and represented simulated deflection basins for a system having the assigned elastic properties. Thus, "basin matching" involved a series of iterations wherein adjustments to the elastic properties were made based on comparisons between the measured and computed basins. This basin-fitting process was similar to conventional static basin fitting, except that the effects of wave propagation were included in each computed basin.

Because the magnitude of the required computational effort necessary for each measured basin exceeded the ability of simple microcomputers, the Cray Supercomputer at The University of Texas was employed for the dynamic analyses described above.

CHAPTER 3. THE SENSITIVITY OF COMPUTED DEFLECTION BASINS TO LAYER MODULI AND BEDROCK DEPTH

INTRODUCTION

Methods for backcalculating layer moduli from FWD measurements rely on the fact that the shape and the depth of static deflection basins are sensitive to the moduli and thicknesses of individual layers. Thus, it is useful to understand qualitatively the relation between computed deflections, layer moduli, and layer thicknesses. This chapter, which is based on forward analysis rather than on backcalculation, presents results from a simple investigation of these qualities for Embankment SW.

A general summary of the effects of modular ratios, layer thicknesses, and load distribution upon stress and strain (with emphasis on the axis of symmetry) was presented by Nielsen (Ref 11), who utilized layer theory adapted from Burmister (Ref 3). However, during backcalculation of layer moduli with FWD data, only the pavement surface deflections are of direct initial interest. The following sections provide an overview of the relation between deflection and layer moduli for hypothetical variations of layer moduli within the profile constructed for Embankment SW.

The pavement profile of Embankment SW consisted of 7 inches of asphalt concrete, 6 inches of crushed limestone (Flexbase), and a very stiff subgrade of compacted select rock fill. Deflection basins were computed with ELSYM5 using static linear-elastic theory; *dynamic effects are not considered.* The results illustrate static deflection behavior for variations in moduli within the layer thicknesses of Embankment SW.

VARIED MODULI WITH CONSTANT SUBGRADE THICKNESSES

To review the relation between basin shape and individual moduli, a total of 150 analyses were made using combinations of five moduli for the ACP (E1), five moduli for the Flexbase (E2), and six moduli for the compacted fill subgrade (E3). The layer thicknesses were 7, 6, and 180 inches for the asphalt concrete, flexbase, and subgrade, respectively. An infinitely stiff layer was modeled beneath the subgrade.

Figures 3.1, 3.2, and 3.3 present computed deflection basins for simulations in which E1, E2, and E3 were individually varied. Several characteristics of layered-system behavior are evident in these plots. In Fig 3.1, Young's

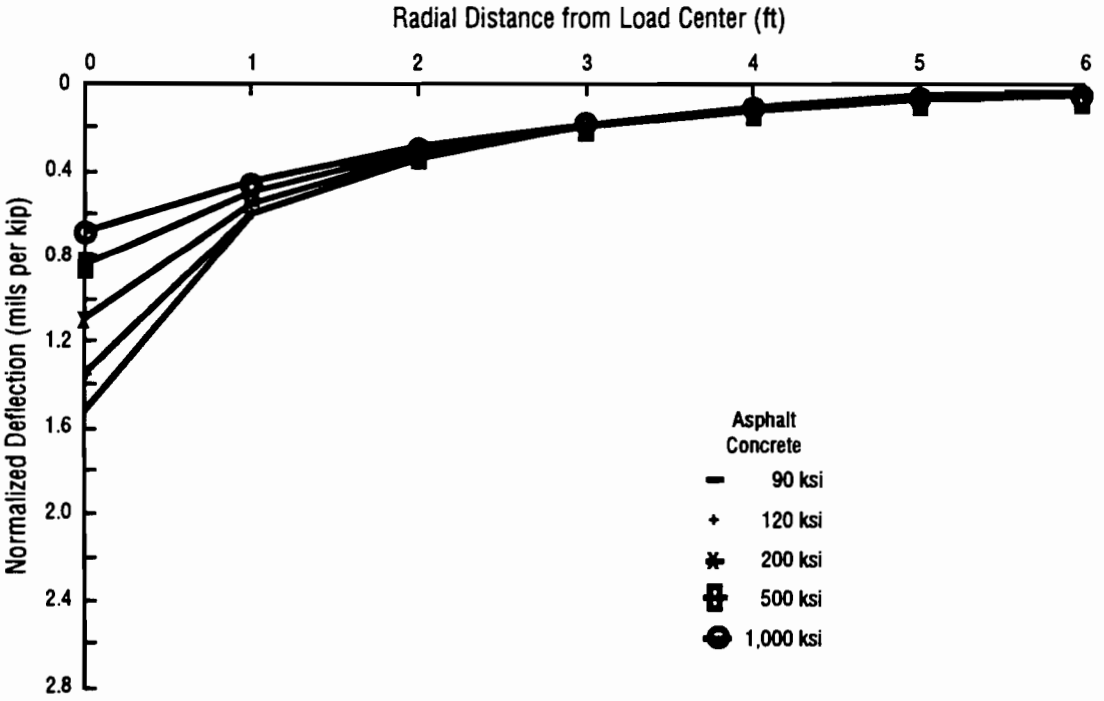

Fig 3.1. Computed deflection versus radial distance with variation in Young's modulus of the asphalt concrete.

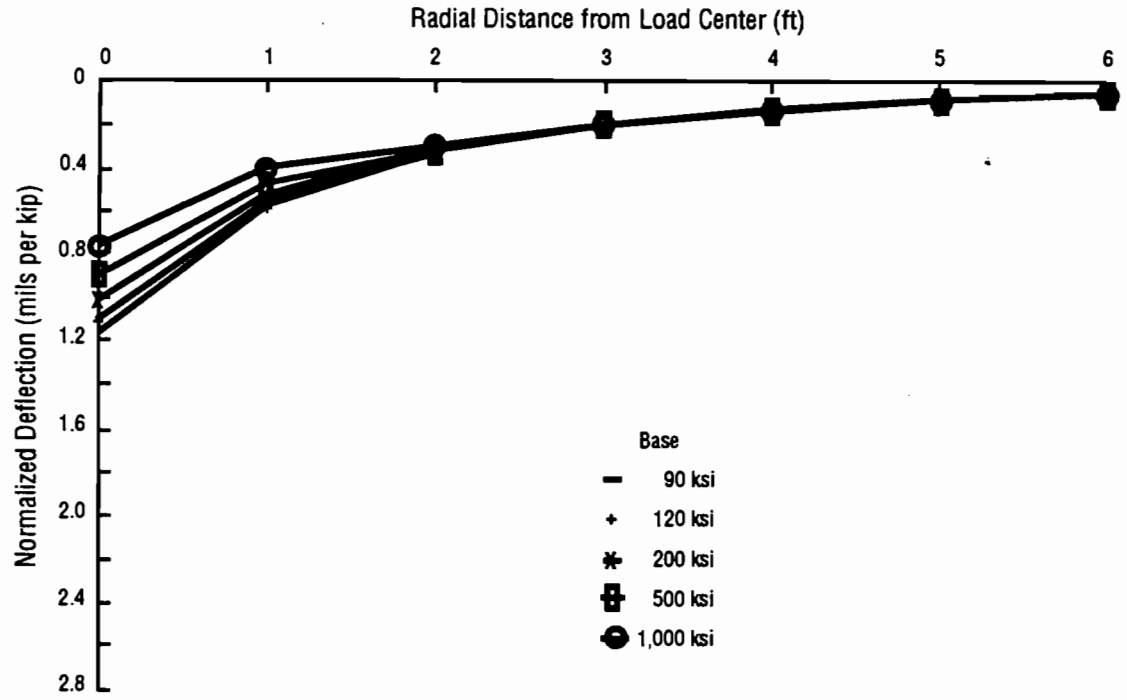

Fig 3.2. Computed deflection versus radial distance with variation in Young's modulus of the base.

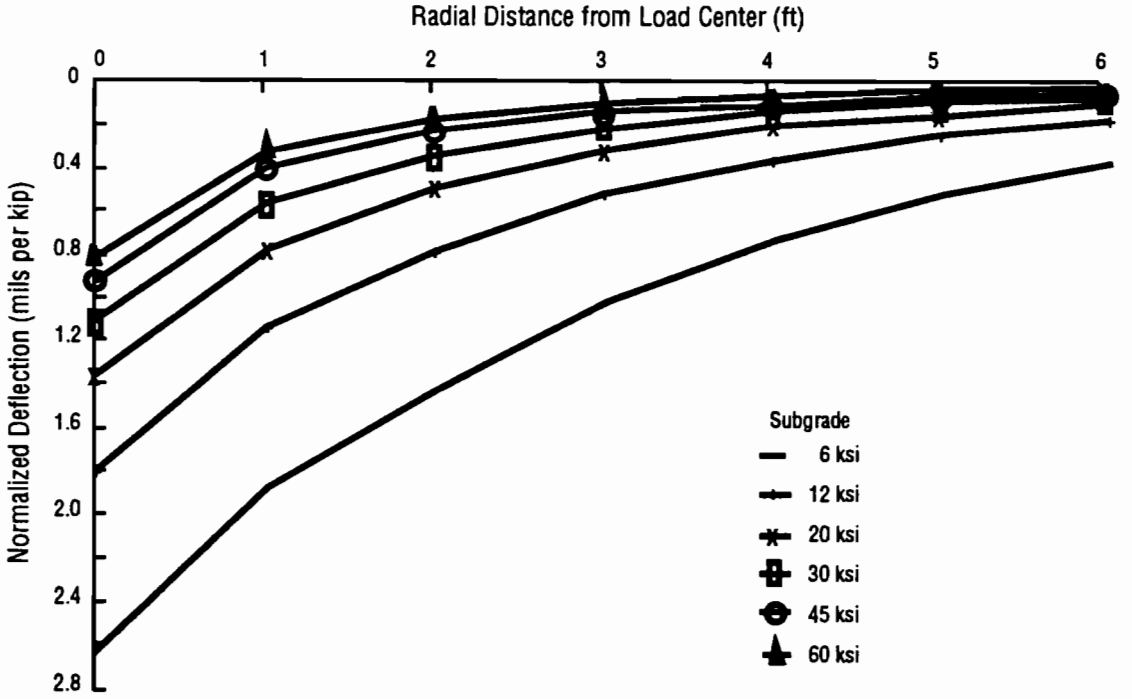

Fig 3.3. Computed deflection versus radial distance with variation in Young's modulus of the subgrade.

modulus of the upper 7-inch layer, E1, is varied from 90 to 1,000 ksi. The modulus of this upper layer has a negligible effect upon surface deflections 2 or more feet from the load center. However, the value of E1 has a very significant effect on the slope of the basin for radii less than 1 foot; higher values of E1 caused a wider distribution of load with shallower and flatter basins.

Computed deflections basins for varied values of Young's modulus in the 6-inch-thick base are plotted in Fig 3.2. Deflections beyond a radius of 2 feet are relatively insensitive to E2. For radii less than 2 feet, E2 affects the slope of the basin. However, for these short radii, the basin slope and depth are more sensitive to modulus of the surface layer than to the modulus of the base.

The variation in computed basins for subgrade moduli from 6 to 60 ksi is shown in Fig 3.3. Because the subgrade modulus is the lowest modulus, and the subgrade is the thickest layer, this modulus has a significant effect upon the total area between the basin and the zero deflection line. Moreover, the subgrade stiffness heavily influences surface deflections for all radial distances and significantly influences the slope of the basin for radii greater than 1 foot.

Thus, for the stiffer subgrade moduli, the percentage change in deflections at a 6-foot radius is nearly proportional to the percentage change in subgrade moduli at this site. However, for small loads, the variation in these deflections is small relative to the measurement accuracy of a standard FWD. Thus, such differences in absolute deflections would be difficult to resolve. (Specifications for the Dynatest 9000 reported an absolute deflection accuracy of 2 percent ± 0.08 mils.)

The above observations of this layered system can be summarized as follows:

(1) The modulus of the 7-inch-thick surface layer has a significant effect on the depth of the basin for radii of 2 feet or less.

(2) The modulus of the 7-inch-thick surface layer heavily influences the slope of the basin for radii of 2 feet or less.

(3) Variations in the stiffness of the 6-inch-thick base affect the basin for radii less than 2 feet. The pattern of such effects is similar to the pattern caused by variation of surface layer stiffness.

(4) Deflection variations due to changes in the base are smaller in magnitude than those due to equal changes in the surface layer. Thus, changes in the base may be difficult to separate from changes in the other layers.

(5) For all but the softest subgrade moduli, the slope of the basin at small radii is only slightly affected by the subgrade moduli.

(6) The overall area between the basin plot and a horizontal line of zero deflection is most influenced by the subgrade stiffness—that is to say, surface deflections at all radii are sensitive to the stiffness of the subgrade.

(7) At a radial distance of 5 or more feet from the load center, the absolute deflections are small relative to the measurement accuracy of the FWD. Thus, large test loads may be needed to obtain reasonable accuracy and definition of deflection beyond a radius of 5 feet.

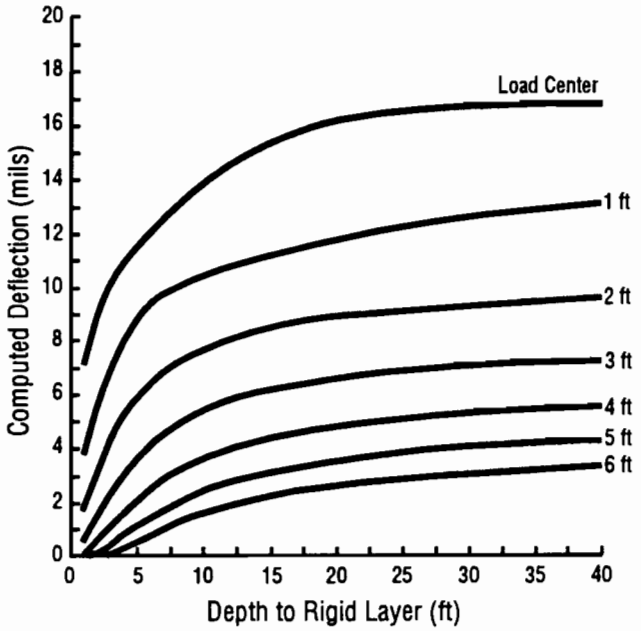

Fig 3.4. Computed deflection versus depth-to-rock for varied radial distances from the load; subgrade modulus is 12 ksi.

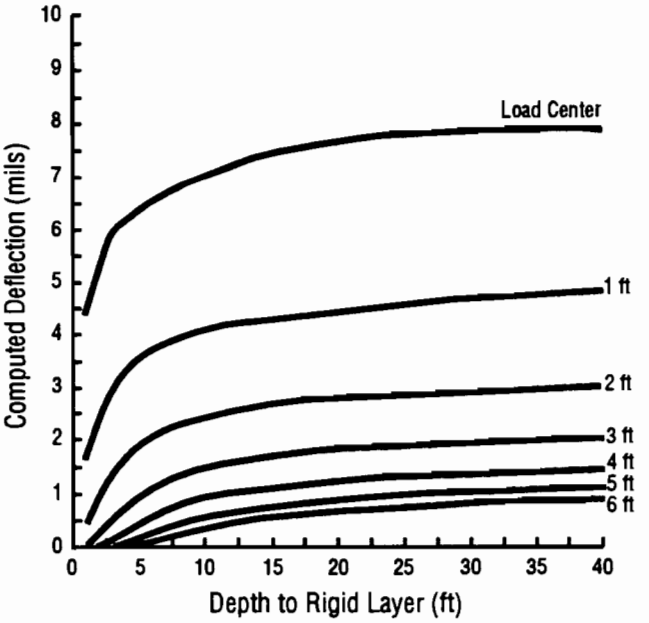

Fig 3.5. Computed deflection versus depth-to-rock for varied radial distances from the load; subgrade modulus is 45 ksi.

VARIED SUBGRADE THICKNESS WITH CONSTANT MODULI

In many circumstances involving shallow bedrock, engineers may not have reliable data regarding the depth of that rock. There may also be uncertainty regarding the relative stiffness of heavily-fissured or weathered rock overlying solid rock. Nevertheless, for static analysis of layered systems, it is necessary to assign a value to the thickness of the subgrade or roadbed overlying the rigid lower boundary of the system. Numerous researchers have investigated the relation between bedrock depth and backcalculated moduli (Refs 13, 14, and 19).

The sensitivity of computed deflections to subgrade thickness for Embankment SW was investigated for depths-to-rock of 1 to 40 feet and subgrade moduli of 12 and 45 ksi. In all cases the load and load radius were 12 kips and 5.91 inches, respectively. Young's moduli of the 7-inch-thick surface and 6-inch-thick base were set to 500 and 200 ksi, respectively. Figures 3.4 and 3.5 present results from these static analyses.

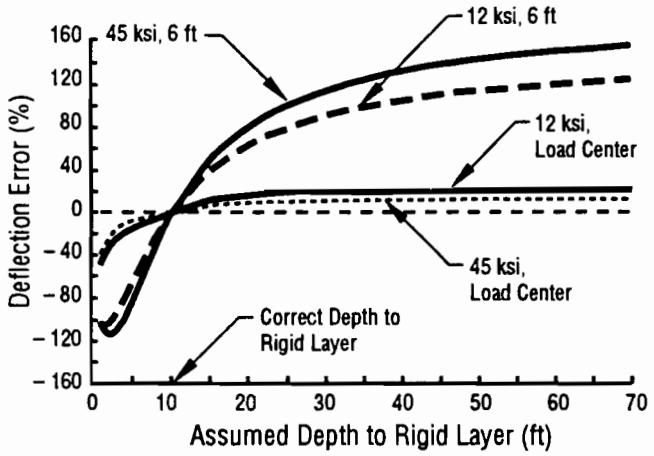

Fig 3.6. Error in computed deflection versus assumed rock depth for radii of 0 and 6 feet and subgrade modulus equal to 12 and 45 ksi. Correct depth-to-rock is 10 feet.

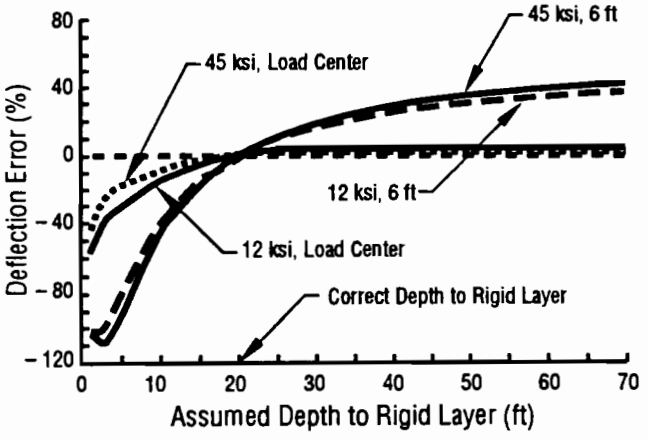

Fig 3.7. Error in computed deflection versus assumed rock depth for radii of 0 and 6 feet and subgrade modulus equal to 12 and 45 ksi. Correct depth-to-rock is 20 feet.

With a subgrade modulus of 12 ksi (Fig 3.4), deflections under the load center do not vary significantly with rock depth when that depth is above a "threshold" of approximately 20 feet. However, deflections decrease by 35 percent (from 17 to 11 mils) as the depth-to-rock decreases from 25 to 5 feet. At a 6-foot radius from the load center, deflections are sensitive to changes in bedrock depth over a greater range of depths. For example, deflections at a 6-foot radius decrease by 11 percent (0.36 mils) as the rock depth decreases from 40 to 25 feet, and they decrease by 83 percent as the rock depth decreases from 25 to 5 feet. When rock is as shallow as 3 feet, negative deflections (upward movement) are computed for a radius of 6 feet.

Results for a subgrade modulus of 45 ksi (Fig 3.5) follow a pattern similar to that described above for the 12-ksi subgrade. However, the threshold rock depth below which load center deflections are relatively insensitive to rock depth is slightly shallower than for the 12-ksi subgrade.

The range of error in static deflections resulting from hypothetical errors in depth-to-rock where the true rock depth is either 10 or 20 feet, as shown in Figs 3.6 and 3.7. These figures highlight the fact that a change in the depth-to-rock causes a significant percentage change in deflections for a radius of 6 feet from the load center. For example, if bedrock is at 20 feet and the assumed rock depth is 15 feet, then a 16-percent under-prediction of deflections would result at a radius of 6 feet.

The following observations were made from the static analyses of Embankment SW with variable rock depths:

(1) When the depth-to-rock is less than a "threshold" value, computed static deflections are sensitive to rock depth.

(2) The threshold depth depends on the radii and subgrade modulus for which deflections are computed. Threshold depths are deepest for large radii and low subgrade moduli.

(3) Underestimation of rock depth would result in smaller computed deflections. During static basin matching, such an error would result in an overestimation of the effective moduli above the rock.

(4) When deflections over shallow rock are normalized (divided by) the deflections over very deep rock, the normalized variation increases with radii. Thus, deflections at larger radial distances which are most sensitive to subgrade modulus are also most sensitive to rock depth.

DYNAMIC ANALYSES WITH VARIABLE DEPTH-TO-ROCK

Under certain conditions, dynamic and static analyses may yield significantly different surface deflections. Shao, Roesset, and Stokoe (Ref 12) investigated this problem with the UTPV computer program for dynamic analysis of pavement systems. Their work showed how resonance within the pavement system can amplify surface deflections. In particular, large amplifications occurred if the frequency of surface excitation lies between the system's fundamental frequency in shear and dilatation. They also showed cases in which such amplification caused large errors in layer moduli backcalculated with static analyses.

The thickness and elastic properties of the subgrade usually control the fundamental frequency. (The fundamental frequency is the frequency at which first-mode resonance occurs.) Thus, for most pavement systems, dynamic amplification depends on (1) the frequency of excitation, (2) the subgrade thickness, and (3) the elastic properties of the subgrade. Field equipment such as the Dynaflect or Road Rater excite pavements with a single frequency and are thus susceptible to resonance. Because a FWD distributes most of its impact energy between 2 and 40 Hz (Fig 2.3), calculation of resonance is more complex—but resonance does occur. As a result, reflected shear and dilatational waves still cause static and dynamic deflections to differ in the FWD test.

Dynamic surface deflections for Embankment SW under FWD loads were computed with the UTPV computer program and compared with static deflections. For these computations, Young's moduli of the surface, base, and subgrade were 700, 75, and 75 ksi, respectively. Subgrade thickness was varied from 7.5 to 110 feet, and an infinitely thick rock layer with a Young's modulus of 890 ksi was placed beneath the subgrade. The ratio of dynamic to static deflections is called the *dynamic amplification factor.*

Figure 3.8 presents computed dynamic amplification factors versus subgrade thickness for various radial distances from the load center. At the load center the amplification factor is relatively small. However, the amplification factor increases with radial distance from the load, and, it is greatest for the largest radial distance. At radii of 1 and 6 feet, maximum values of the amplification factor are 1.05 and 1.65, respectively. These maximum amplification factors occur for subgrade thicknesses near 12.5 feet. The variations and magnitudes of these amplification factors are large relative to the variation of static deflections (Figs 3.4 and 3.5) with subgrade thickness. Thus, in a rigorous dynamic analysis, deflections may be very sensitive to subgrade thickness. This is especially true for radial distances of 3 or more feet from the load center.

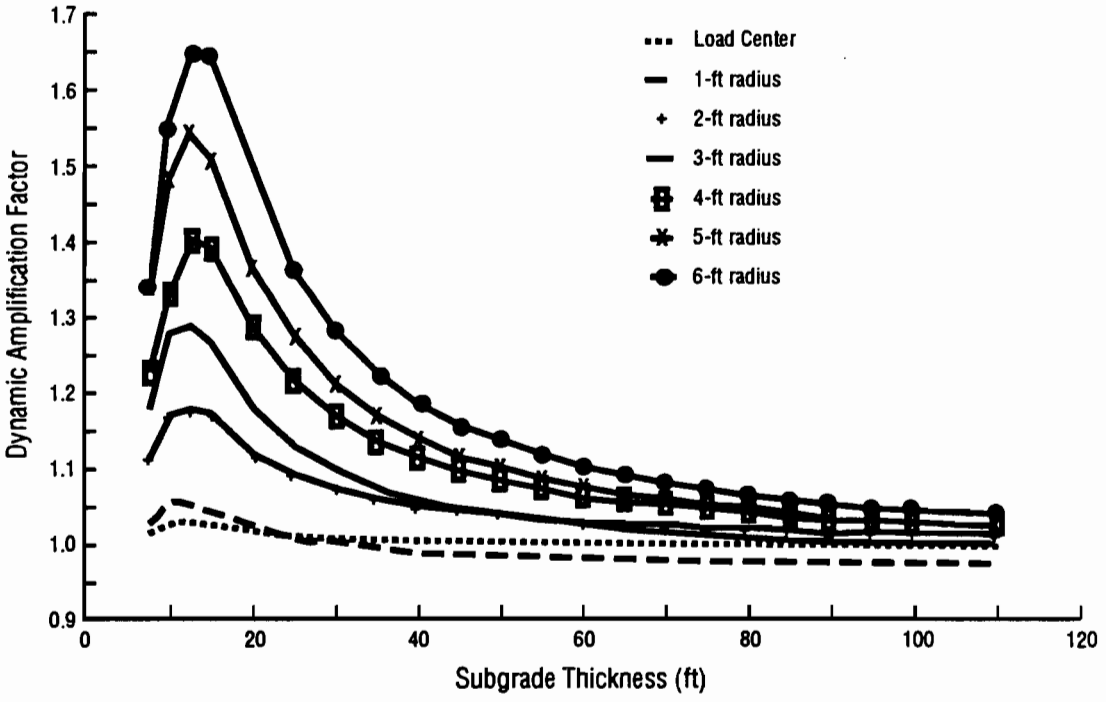

Fig 3.8. Dynamic amplification factor versus subgrade thickness for varied radii.

CHAPTER 4. THE SENSITIVITY OF BACKCALCULATED LAYER MODULI TO ERRORS IN DEFLECTION MEASUREMENT OR BEDROCK DEPTH

INTRODUCTION

Backcalculation of layer moduli from FWD deflections is an indirect approximate procedure. One basic approach common to all published backcalculation programs involves comparing many directly-computed basins with a measured basin. The result of these comparisons is a selected set of moduli that yield a computed basin which most closely matches the measured basin. When a computed basin matches the measured basin, the moduli used for the computed basin are accepted as a representation of field conditions. This chapter investigates the accuracy of a backcalculation program, as well as the sensitivity of backcalculated moduli to errors in deflection measurement.

Conventional basin fitting uses static elastic layer theory to model the relation between basins and layer moduli. This model provides a unique relation between computed basins and moduli, but neglects the dynamic aspects of FWD loading. Dynamic analysis is less common and requires significantly more computer time than static analysis. However, significant differences sometimes exist between static and dynamic analyses. This report uses the MODULUS computer program from the Texas Transportation Institute (Ref 7) for static analysis, and the UTPV computer program (Ref 8) for dynamic analysis.

Regardless of the model used to compute deflections, several practical difficulties or limitations are inherent in backcalculation. For instance, an infinite number of trial combinations of moduli are conceivable, thus rendering difficult the efficient selection of trial moduli and rapid computation of basins. Moreover, methods chosen to solve these problems can cause uncertainty and can lead to general or imprecise results. Other problems relate to the facts that (1) measured basins are subject to measurement error; (2) assumed layer thicknesses may be incorrect; and (3) the theoretical model of deflection behavior always involves simplifying assumptions. Thus, a perfect match between computed and measured deflections is not possible. The choice of the best match depends on the selection criteria.

The following sections discuss results of the MODULUS program for (1) theoretically-computed basins, (2) basins with known deflection errors, and (3) profiles with errors in depth-to-rock. All analyses use the basic pavement profile of Embankment SW, as discussed in Chapter 1.

BACKCALCULATION WITH MODULUS

The backcalculation procedure used in MODULUS is based on the assumption, from linear elasticity, that the computed deflection, w_i, at radius r_i, is uniquely related to other variables as follows:

$$w_i = f_i(E_k, \nu_k, h_k, r_k, O) \tag{4.1}$$

where

E_k, ν_k = modulus of elasticity and Poisson's ratio of the k^{th} layer (k=1 to N),
E_{sg} = modulus of elasticity of the subgrade,
h_k = thickness of layer k,
r_k = ratio of any layer modulus over subgrade modulus (E_{sg}), and
O = other variables such as load, contact area, etc.

During backcalculation, the modular ratios E_k/E_{sb} are unknown. The subgrade modulus of elasticity, E_{sg}, is also unknown, but it is inversely proportional to deflection. Moreover, deflection is linearly proportional to load, P, and is a unique function of the modular ratios, E_k/E_{sg} (k = 1 to n-1 for n layers):

$$w_i = \frac{P}{E_{sg}} f\left[\frac{E_1}{E_{sg}}, \frac{E_2}{E_{sg}}, \ldots \frac{E_k}{E_{sg}}\right] \tag{4.2}$$

The basin-fitting subroutine in MODULUS minimizes the squared error, e^2, between computed and measured deflection in the following objective function:

$$e^2 = \sum_{i=1}^{s} \left(1 - \frac{w_i}{D_i}\right)^2 m_i \tag{4.3}$$

where

s = number of deflection data points,
D_i = measured deflection for the i^{th} data point, and
m_i = weighing factor for the i^{th} data point.

For most standard configurations of FWD geophones, the program authors recommend equal weighting factors for m_i (Ref 7).

Before searching for a solution that minimizes the objective function, MODULUS computes deflections for a matrix of modular ratios. Ratios in this matrix bracket assume the range of moduli values specified by the operator. For a typical three-layer system, the matrix is usually 3 x 3 and thus requires computation of nine basins using static linear elastic theory. A four-layer system would use a matrix of at least 3 x 3 x 3. The version of MODULUS used for this report employed the Chevron elastic layer program to compute basins for the data bank. After storing computed deflections in a data bank, MODULUS orders a search routine to minimize the objective function. MODULUS computes the individual value for the objective function by comparing the measured basin with basins in the matrix or basins interpolated from the matrix.

MODULUS typically requires less computation and operator time than FPEDD (Ref 5) and BISDEV (Ref 6) when fitting two or more basins with the same profile of layer thicknesses. The search routine requires only a small fraction of the time used to build the data bank. Thus, additional basins are fit with little increase in total computation time. Basin fitting for this report was done with a microcomputer having a 80387 processor and a clock speed of 20 MHz. Total computation time for fitting 28 basins with the same thickness profile was typically 8 to 15 minutes. This relatively fast rate of basin fitting is one advantage of the MODULUS program.

Eight deflection basins computed with the ELSYM5 program were used to test the performance of the MODULUS program. Layer thicknesses were 7, 6, and 180 inches for the surface, base, and subgrade, respectively. ELSYM5 modeled a rigid rock layer beneath the subgrade. This basic profile is that of RAMP SW. However, the individual layer moduli used for computing each basin differed, as shown in Table 4.1.

The ELSYM5 program and the CHEVRON program used in MODULUS gave essentially similar deflections for all eight cases. Thus, the moduli backcalculated by MODULUS indicated the uncertainty associated with backcalculation itself. Use of computed basins eliminated uncertainty due to external problems such as model assumptions or deflection error.

Results from this backcalculation test appear in Table 4.1. The MODULUS program provided excellent results for the 6-inch-thick surface layer and the 180-inch-thick subgrade. The Match Quality Index, MQI, is the average percentage difference between the computed and measured basins. Values for the MQI appear in Table 4.1; in all but one case the MQI was less than 1.0 percent.

For the base layer, the ratio between backcalculated and actual moduli ranged from 0.69 to 0.99 and averaged 0.86. The large error associated with backcalculated base moduli suggests that the analysis is insensitive to the base moduli. This finding is consistent with the results from forward modeling that are presented in Chapter 3.

Overall, the MODULUS results for Embankment SW (Table 4.1) suggest that the backcalculation algorithm and program are accurate. However, significant errors in backcalculated surface and subgrade moduli may originate from other sources, which are discussed below.

DEFLECTION MEASUREMENT ERROR

Errors in deflection measurements may affect backcalculation in two ways. First, the backcalculated moduli may directly reflect the measurement error. For example, a measured basin that is too deep at the farthest receivers will result in an underestimation of the subgrade modulus. Second, errors that distort the basin from a shape that can be computed by a given theoretical

TABLE 4.1. PERFORMANCE OF MODULUS TEST PROGRAM; REFERENCE AND BACKCALCULATED MODULI

Actual Moduli Used in ELSYM5 (ksi)			Backcalculated Moduli from MODULUS Program (ksi)				Ratio of Backcalculated Moduli to Reference Moduli		
Surface	Base	Subgrade	Surface	Base	Subgrade	Match Quality Index %	Surface	Base	Subgrade
200	90	6.0	186	62	6.2	3.6	0.93	0.69	1.03
200	90	20.0	205	82	20.3	0.7	1.03	0.92	1.01
500	90	20.0	550	72	20.2	0.5	1.10	0.80	1.01
120	120	20.0	122	116	20.6	0.7	1.02	0.96	1.03
500	120	20.0	539	99	20.2	0.5	1.08	0.82	1.01
500	120	30.0	526	101	30.1	0.5	1.05	0.84	1.00
500	120	45.0	518	107	45.7	0.3	1.04	0.89	1.02
500	120	60.0	501	119	61.4	0.5	1.00	0.99	1.02
					Average Ratio	0.9	1.03	0.86	1.02
					Standard Deviation	0.1	0.032	0.067	0.008

model will complicate the search for a minimum of the objective function.

The effect of deflection errors upon backcalculation was studied using hypothetical distortions of two correct theoretical basins. These reference basins were labeled Case 1A and Case 2A. Following the basic profile of Embankment SW, the surface, base, and subgrade thicknesses were 7, 6, and 180 inches, respectively. Reference moduli for the surface, base, and subgrade were 200, 90, and 20 ksi, respectively for Case 1A. For Case 2A, the reference moduli were 500, 90, and 45 ksi, respectively. Backcalculated moduli for Cases 1A and 2A (without distortions) were very close to the reference moduli, as shown in Table 4.2.

According to the performance specifications for the Dynatest 9000 FWD, an absolute deflection accuracy is 2 percent ±0.08 mils, and deflection resolution is 0.4 mils. Independent investigations (Ref 1) of an earlier FWD model using similar geophones reported an error of 2 to 8 percent. Considering this realm of measurement uncertainty, three hypothetical basin distortions were defined.

The first distortion (Cases 1B and 2B in Table 4.2) is simply the correct deflection plus 4 percent and 0.4 mils. Thus, if ELSYM5 computes a 20-mil deflection, then the distorted value becomes 21.2 mils. Cases 1C and 2C represent the correct basin reduced by 4 percent and 0.4 mils. The third distortion (Cases 1D and 2D) is a sawtooth combination of the errors for the other cases. Beginning with the deflection at the load plate and extending outward, the errors for Cases 1C and 2C were -(4 percent + 0.4 mils), 0 percent, +(4 percent + 0.4 mils), 0 percent, -(4 percent + 0.4 mils), etc.

Backcalculated layer moduli for each distorted basin appear in Table 4.2. For the 6-inch base, the ratio of backcalculated to reference moduli ranged from 0.1 to 5.2, and the ratio was never close to unity. This behavior shows that backcalculated base moduli are extremely sensitive to measurement error in the pavement system analyzed. The surface and subgrade fare better than the base. For Case 1B these two layers are within 15 percent of the reference value. For Case 2B the surface and subgrade are within about 30 percent of the reference value.

The sawtooth pattern of deflection error defined by Cases 1D and 2D provided reasonable estimates of subgrade moduli. However, backcalculated surface moduli were 1.7 to 1.9 times higher than the reference moduli. This behavior suggests that surface modulus is sensitive to the slope of the basin between the load center and a 1-foot radius. These results reflect the fact that the sawtooth error reduced deflections at the load center and reduced the slope of the basin between the 0- and 1-foot radii. As shown in Chapter 3, this reduced slope is associated primarily with stiffer surface layers.

The results shown in Table 4.2 reflect the results of measurement errors that are slightly larger than the errors expected from careful operation of the Dynatest 9000 FWD. However, the results show that backcalculation is not robust toward measurement errors. When deflections are small (owing to low loads and stiff pavements), typical percentage errors may resemble Cases B, C, and

TABLE 4.2. MODULI BACKCALCULATED WITH PROGRAM "MODULUS" USING HYPOTHETICAL MEASUREMENT ERRORS

(A) REFERENCE MODULI: SURFACE = 200, BASE = 90, AND SUBGRADE = 20 KSI

	Backcalculated Moduli (ksi)				Ratio of Backcalculated Moduli to Reference Moduli		
Case	Surface	Base	Subgrade	Match Quality Index %	Surface	Base	Subgrade
1A	199	86	20	0.5	1.0	1.0	1.0
1B	170	150	17	3.3	0.9	1.7	0.9
1C	775	8	30	7.7	3.9	0.1	1.5
1D	388	37	21	9.1	1.9	0.4	1.0

(B) REFERENCE MODULI: SURFACE = 500, BASE = 90, AND SUBGRADE = 45 KSI

	Backcalculated Moduli (ksi)				Ratio of Backcalculated Moduli to Reference Moduli		
Case	Surface	Base	Subgrade	Match Quality Index %	Surface	Base	Subgrade
2A	559	98	46	1.6	1.1	1.1	1.0
2B	337	465	34	6.8	0.7	5.2	0.7
2C	1,911	13	129	24.7	3.8	0.1	2.9
2D	828	37	54	21.6	1.7	0.4	1.2

D above. Under such conditions the backcalculated properties may differ significantly from field properties.

ERRORS IN ASSUMED DEPTH-TO-BEDROCK

Backcalculation programs require values for the thickness of each layer. Yet, while design and construction records or the results from cores can provide this information for surface layers, reliable values for the depth of the rock surface are seldom available. Uddin, Meyer, and Hudson (Ref 13) discussed the significance of this uncertainty. They also presented a simple approximate method to account for the dynamic effects of shallow rock. Briggs and Nazarian (Ref 14) discussed the effects of unknown rock depth on backcalculation and calculated pavement performance. This section presents a study of the sensitivity of the backcalculated moduli to errors in assumed rock depth.

Four reference deflection basins computed with ELSYM5 were the basis of the study. Surface and base moduli were 500 and 200 ksi, respectively; subgrade moduli were 12 and 45 ksi; and the depth-to-rock was 12 and 25 feet. Thus, a total of four cases combining two subgrade moduli and two depths-to-rock were selected, based on values anticipated for the field case study. The four basins computed with these moduli and rock depths were passed to MODULUS with a wide range of errors in the assigned depth-to-rock.

Tables 4.3 and 4.4 summarize results from the MODULUS program. Figures 4.1 to 4.4 present the ratio of computed moduli to reference moduli for the surface and subgrade. These results show that the distance-to-rock must be known within ±2 feet when rock is within 12 feet of the surface. For the basins with a reference rock depth of 25 feet, an uncertainty of 5 feet is acceptable. Note that overestimation of the rock depth provides smaller errors than underestimation.

SUMMARY

The performance of the MODULUS program is quite good relative to the errors generated outside the

TABLE 4.3. RESULTS OF BACKCALCULATIONS WITH VARIED DEPTH-TO-ROCK WITH SUBGRADE YOUNG'S MODULUS = 12 KSI

(A) REFERENCE DEPTH-TO-ROCK = 12 FEET

Modulus Subgrade Thickness (ft)	Backcalculated Young's Modulus (ksi)			Match Quality Index %	Ratio of Backcalculated Moduli to Reference Moduli		
	Surface	Base	Subgrade		Surface	Base	Subgrade
6	684	61.1	20.4	11.5	1.37	0.31	1.70
8	910	47.1	15.7	3.7	1.82	0.24	1.31
10	981	64.7	13.4	1.1	1.96	0.32	1.12
12	502	196.0	12.2	0.1	1.00	0.98	1.02
15	297	437.0	11.0	1.3	0.59	2.19	0.92
20	210	973.0	10.0	2.8	0.42	4.87	0.83
25	230	933.0	9.3	3.7	0.46	4.67	0.78
30	250	888.0	8.9	4.4	0.50	4.44	0.74
40	351	587.0	8.5	5.0	0.70	2.94	0.71
50	373	569.0	8.2	5.0	0.75	2.85	0.69
60	394	548.0	8.1	4.8	0.79	2.74	0.67
70	405	546.0	7.9	4.6	0.81	2.73	0.66

(B) REFERENCE DEPTH-TO-ROCK = 25 FEET

Subgrade Thickness (ft)	Backcalculated Young's Modulus (ksi)			Match Quality Index %	Ratio of Backcalculated Moduli to Reference Moduli		
	Surface	Base	Subgrade		Surface	Base	Subgrade
12	1,694	5.0	18.3	2.1	3.39	0.03	1.53
15	1,493	11.5	15.0	2.1	2.99	0.06	1.25
20	569	157.0	12.8	1.0	1.14	0.79	1.07
25	507	203.0	12.1	0.1	1.01	1.02	1.01
30	541	209.0	11.6	0.8	1.08	1.05	0.97
40	636	200.0	11.0	1.7	1.27	1.00	0.92
50	722	187.0	10.7	1.8	1.44	0.94	0.89
60	818	170.0	10.5	1.7	1.64	0.85	0.88
70	885	161.0	10.3	1.7	1.77	0.81	0.86

backcalculation process itself. External errors include errors in deflection data or errors in layer thicknesses.

Backcalculated moduli are relatively sensitive to errors in deflection measurement. Thus, an increase in the accuracy of the geophones used in the FWD will provide a useful increase in the reliability of backcalculation. The value of increased deflection accuracy is greatest for tests on very stiff pavements or tests with low load levels.

When bedrock is within about 12 feet of the surface, rock depth should be known within ±2 feet. However, when rock depth is 25 feet or more, an uncertainty of up to 5 feet is acceptable. Larger uncertainty in the depth-to-rock will cause significant errors in backcalculated layer moduli.

Based on the results reported in this chapter, backcalculation with the MODULUS program works best for the subgrade layer. Further, results for the subgrade are more robust than results for other layers when deflection errors or subgrade thickness errors are introduced. The favorable sensitivity of backcalculations to subgrade moduli may be due to the fact that the entire surface of the FWD basin is significantly affected by the subgrade stiffness.

The study of sensitivity and error presented in this chapter was based on a static linear elastic model of pavement behavior. Additional types of sensitivity and error will occur with static analysis of dynamic load-deflection data, such as data from the FWD. For example, using the instantaneous peak of a time-varying load may cause error, because the dynamic response to a transient load differs from the static response to a static load equal to the peak of that transient load. Wave propagation phenomena, such as reflections from a rigid layer, will also alter the dynamic load-deflection behavior. Finally, if large strains occur, non-linear stress-strain behavior may cause additional error.

TABLE 4.4. RESULTS OF BACKCALCULATIONS WITH VARIED DEPTH-TO-ROCK WITH SUBGRADE YOUNG'S MODULUS = 45 KSI

(A) REFERENCE DEPTH-TO-ROCK = 12 FEET

Subgrade Thickness (ft)	Backcalculated Young's Modulus (ksi)			Match Quality Index %	Ratio of Backcalculated Moduli to Reference Moduli		
	Surface	Base	Subgrade		Surface	Base	Subgrade
6	1,951	11.0	110.0	7.5	3.90	0.06	2.44
8	1,744	15.9	72.4	6.2	3.49	0.08	1.61
10	1,110	43.6	53.9	4.0	2.22	0.22	1.20
12	507	176.0	46.4	1.0	1.01	0.88	1.03
15	412	308.0	42.2	2.0	0.82	1.54	0.94
20	361	527.0	38.3	5.0	0.72	2.64	0.85
25	368	607.0	36.1	6.6	0.74	3.04	0.80
30	378	656.0	34.6	7.5	0.76	3.28	0.77
40	348	993.0	33.1	9.1	0.70	4.97	0.74
50	366	961.0	32.0	9.2	0.73	4.81	0.71
60	377	942.0	31.4	9.1	0.75	4.71	0.70
70	394	923.0	30.8	9.1	0.79	4.62	0.68

(B) REFERENCE DEPTH-TO-ROCK = 25 FEET

Subgrade Thickness (ft)	Backcalculated Young's Modulus (ksi)			Match Quality Index %	Ratio of Backcalculated Moduli to Reference Moduli		
	Surface	Base	Subgrade		Surface	Base	Subgrade
12	1,539	20.5	64.9	5.4	3.08	0.10	1.44
15	1,199	37.2	55.4	4.3	2.40	0.19	1.23
20	620	130.0	48.1	2.1	1.24	0.65	1.07
25	511	190.0	45.5	0.3	1.02	0.95	1.01
30	497	217.0	43.8	0.9	0.99	1.09	0.97
40	503	248.0	41.8	2.4	1.01	1.24	0.93
50	529	255.0	40.7	2.7	1.06	1.28	0.90
60	540	262.0	40.1	2.8	1.08	1.31	0.89
70	548	273.0	39.5	2.9	1.10	1.37	0.88

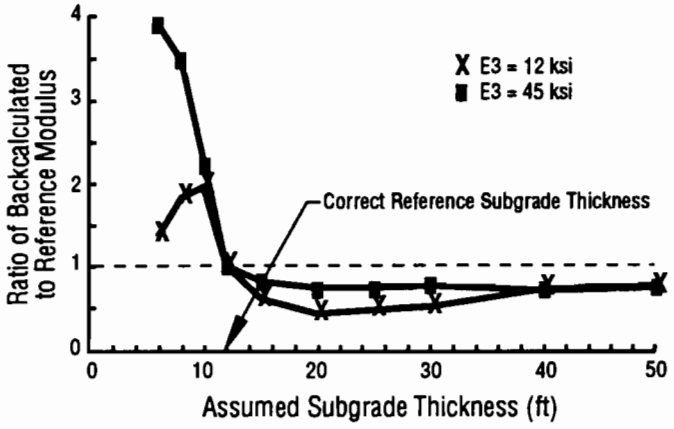

Fig 4.1. Modulus ratio for the surface asphalt concrete with a 12-foot-thick subgrade.

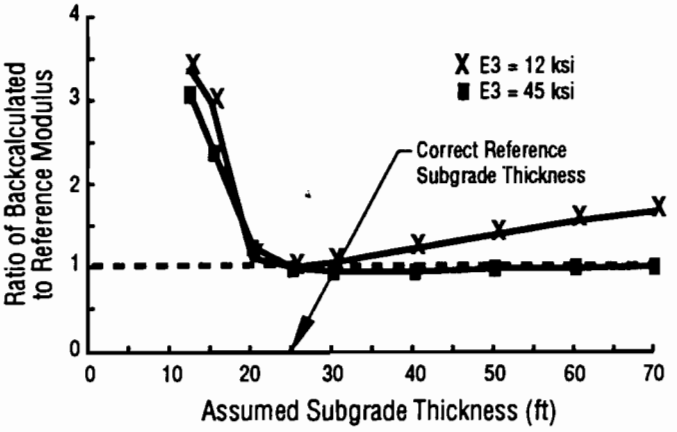

Fig 4.3. Modulus ratio for the surface asphalt concrete with a 25-foot-thick subgrade.

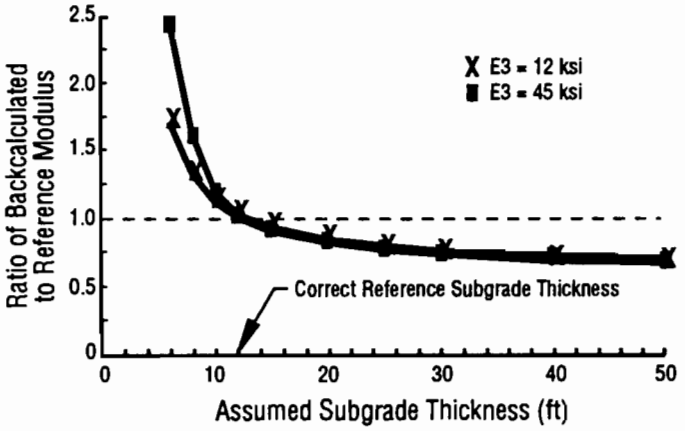

Fig 4.2. Modulus ratio for the subgrade with a 12-foot-thick subgrade.

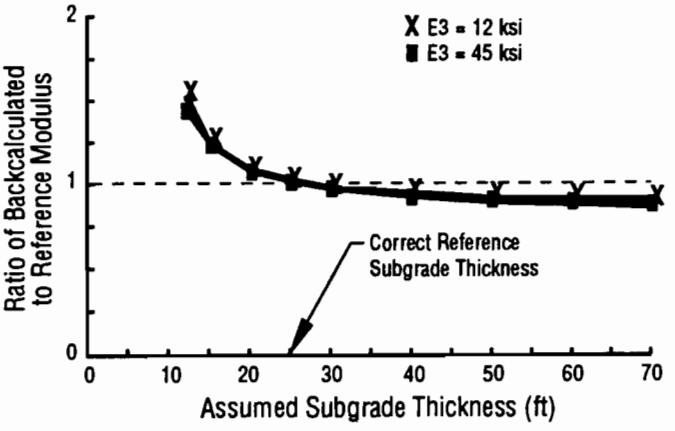

Fig 4.4. Modulus ratio for the subgrade with a 25-foot-thick subgrade.

CHAPTER 5. RESULTS FROM FALLING WEIGHT DEFLECTOMETER TESTS ON EMBANKMENT SW

INTRODUCTION

Deflection data for Embankment SW were measured with a Dynatest 9000 FWD provided by the Texas State Department of Highways and Public Transportation. The embankment received an initial 4-inch-thick course of AC followed (5 days later) with a 3-inch-thick course of AC. Researchers conducted a thorough series of FWD tests on each lift—first during initial cooling of the AC, and then 3 to 4 days after placement of each lift. Seven individual FWD test stations, each spaced 50 feet apart, spanned a 300-foot length of Embankment SW between Stations 275+50 and 278+50 (Fig 1.1). These stations had subgrade thicknesses of 7 to 20 feet. All FWD tests were made on the centerline of the embankment.

Thermocouples monitored the temperature of the asphalt concrete at four depths. One additional thermocouple monitored the temperature of the base approximately 1 inch below the AC. Temperature data for May 29 and June 3 are shown in Figs 5.1 and 5.2. Temperature varied with depth and time in a pattern similar to that found by E. S. Barber (Ref 15). In this case study, reported temperature values for the AC are usually the average of values measured in the asphalt during the test.

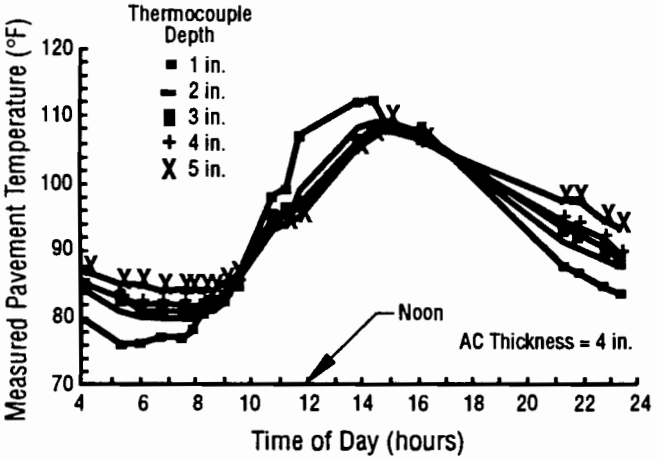

Fig 5.1. Pavement temperatures for May 29, 1989.

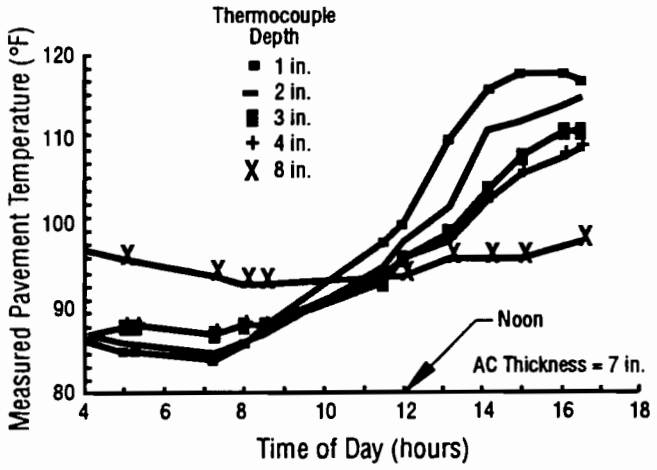

Fig 5.2. Pavement temperatures for June 3, 1989.

Individual tests at each station included a programmed sequence of at least 26 drops. Loads ranged from 7 to 28 kips. Data in the first eight columns of Table 5.1 illustrate the load sequence and measurements for a typical test. However, for clarity of presentation, most FWD deflection data were normalized to a load of 1 kip by dividing the recorded peak load into the recorded deflection. Figure 5.3 is a plot of normalized basins obtained from four different loads at Station 276+50 with 7 inches of AC. For loads of 7 to 25 kips, deflection near the load center was linearly related to load. For the longest radial distances, deflections increased slightly faster than proportional loads. This behavior was typical for other tests, regardless of AC temperature, AC thickness, or subgrade thickness.

Plotted deflection basins typically represent an average of three or four normalized basins at a given station. Such basins were averaged from sequential drops with loads ranging from 8 to 13 kips. However, measurements from different stations or under different conditions were not averaged together.

Normalized deflection basins for tests at all stations and an AC thickness of 7 inches are shown in Fig 5.4. The field measurements of these basins—taken during a relatively short morning period, with AC temperature ranging between 86°F and 88°F—illustrate the variation of deflection basins along the 300-foot section with varied depth-to-rock. Figure 5.5 presents the same deflection data plotted as deflection versus depth-to-rock for different radial distances (different geophone locations). A similar pattern occurs in Fig 5.6 for 4-inch and 7-inch total AC thicknesses.

LAYER MODULI FROM STATIC ANALYSIS

The last three columns of Table 5.1 list layer moduli backcalculated with MODULUS for the 28 sequential drops at Station 276+50. Coefficients of variation for the AC, base, and subgrade were 0.07, 0.12, and 0.05, respectively. Three interesting patterns appear in these backcalculated moduli:

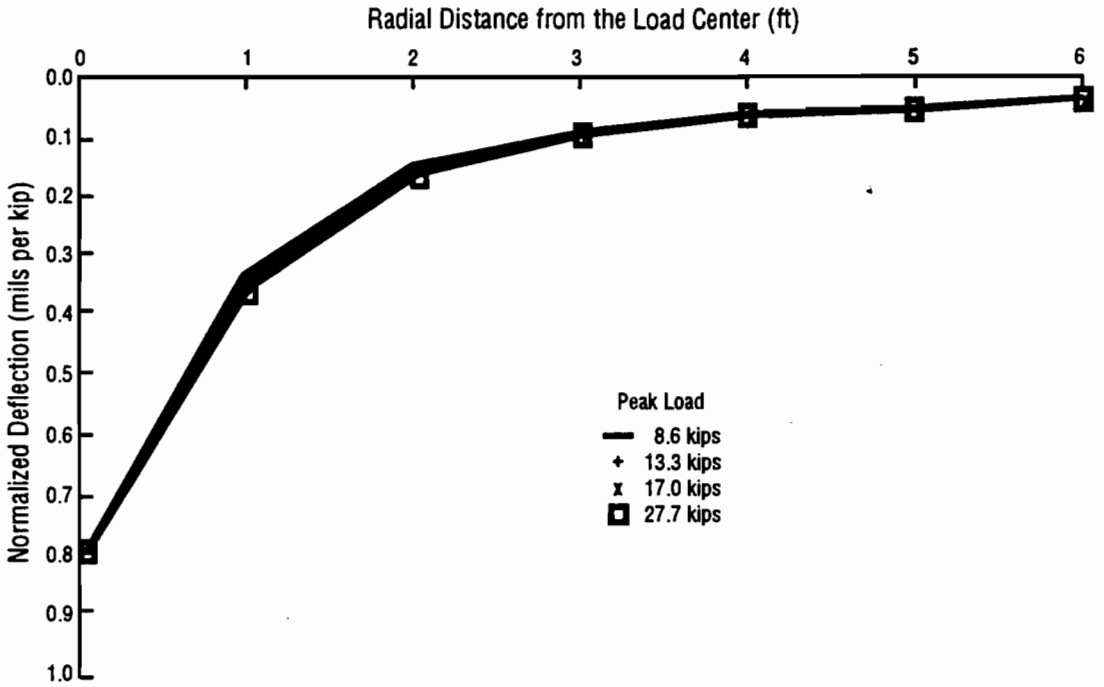

Fig 5.3. Normalized deflection basins for tests at four load levels at Station 276+50 with 7 inches of AC.

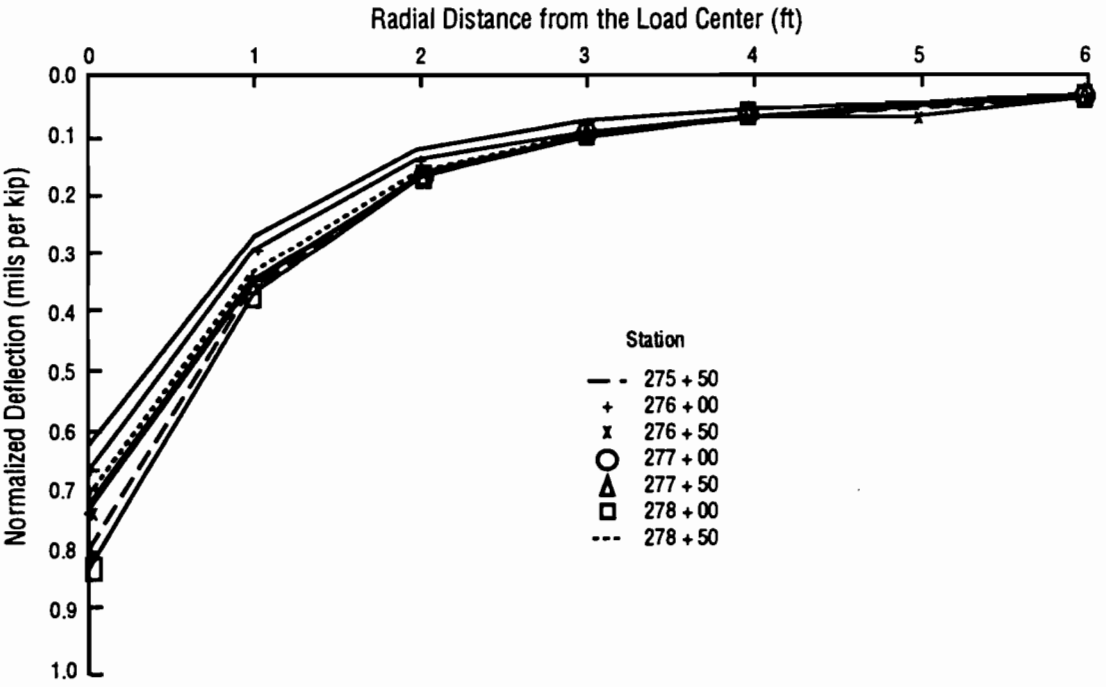

Fig 5.4. Normalized deflection basins for seven stations with 7 inches of AC and temperatures ranging between 86 and 88°F.

TABLE 5.1. FIELD RESULTS AND BACKCALCULATED LAYER MODULI FROM FALLING WEIGHT DEFLECTOMETER TESTS AT STATION 276+50, JUNE 3, 1989

Peak Load (kips)	Under Load	Deflection in Mils at Sensor Locations						Layer Moduli Backcalculated with MODULUS (kips)		
		12 in.	24 in.	36 in.	48 in.	60 in.	72 in.	AC	Base	Subgrade
8,811	7.15	2.83	1.24	0.83	0.57	0.47	0.35	187	135	62
13,459	10.89	4.51	2.02	1.30	0.91	0.74	0.54	199	130	60
17,074	13.74	5.85	2.66	1.69	1.21	0.95	0.73	210	134	58
25,702	21.52	9.44	4.23	2.67	1.88	1.49	1.18	215	114	55
8,628	7.06	2.87	1.28	0.84	0.59	0.50	0.37	189	142	59
8,541	6.91	2.85	1.22	0.81	0.56	0.47	0.33	195	123	62
8,589	6.89	2.81	1.22	0.80	0.53	0.46	0.33	198	123	62
8,601	6.87	2.81	1.22	0.80	0.53	0.43	0.31	201	112	64
13,276	10.62	4.54	2.90	1.30	0.92	0.74	0.53	215	126	59
13,304	10.66	4.59	2.90	1.31	0.93	0.76	0.54	216	126	58
13,288	10.62	4.57	2.07	1.31	0.93	0.75	0.54	215	128	58
13,240	10.55	4.55	2.10	1.30	0.93	0.76	0.54	219	129	58
16,983	13.46	5.90	2.69	1.69	1.21	0.95	0.72	225	128	58
16,971	13.44	5.93	2.67	1.70	1.23	0.97	0.74	227	131	57
16,935	13.40	5.93	2.67	1.70	1.23	0.97	0.75	227	132	57
16,915	13.37	5.94	2.67	1.70	1.22	0.98	0.76	230	131	57
25,790	20.68	9.28	4.24	2.65	1.85	1.44	1.12	235	116	56
25,686	20.72	9.31	4.29	2.69	1.90	1.48	1.17	234	120	55
25,659	20.72	9.24	4.33	2.67	1.87	1.46	1.15	234	120	55
25,678	20.64	9.35	4.24	2.69	1.89	1.48	1.17	236	121	55
8,295	6.77	2.78	1.18	0.74	0.48	1.35	0.26	222	73	68
13,117	10.70	4.62	2.02	1.26	0.88	0.68	0.50	220	98	60
16,848	13.55	5.99	2.67	1.68	1.20	0.94	0.71	226	116	58
25,790	20.67	9.31	4.31	2.68	1.941	1.50	1.19	236	125	55
8,342	6.97	2.92	1.25	0.83	0.56	0.46	0.34	196	112	59
8,307	6.84	2.87	1.20	0.81	0.55	0.43	0.30	196	107	62
8,330	6.81	2.89	1.20	0.80	0.54	0.44	0.30	203	102	62
8,330	6.77	2.85	1.21	0.79	0.54	0.45	0.30	203	106	62
					Mean			215	120	59
					Standard Deviation			15	14	3
					Coefficient of Variation			0.07	0.12	0.05

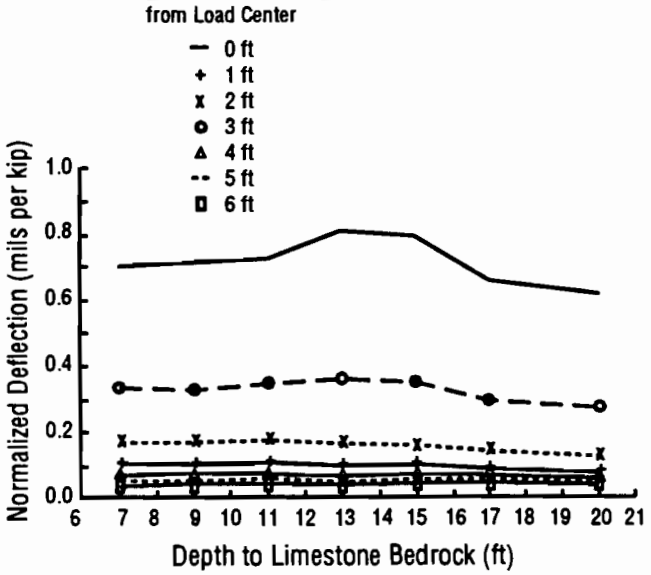

Fig 5.5. Normalized deflection versus subgrade thickness for varied distances from the load center.

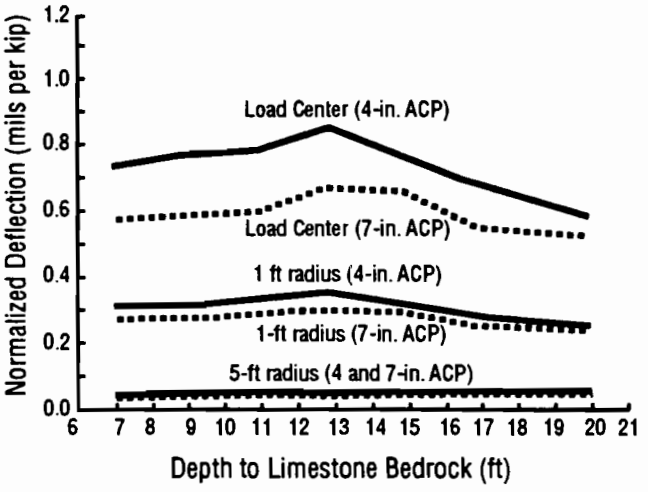

Fig 5.6. Normalized deflection versus subgrade thickness for two radii and two AC thicknesses.

TABLE 5.2. COMPARISON OF YOUNG'S MODULI BACKCALCULATED FROM FWD DATA WITH 4 AND 7 INCHES OF AC USING THE

	Station Number	275 + 50	276 + 00	276 + 50	277 + 00	277 + 50	278 + 00	278 + 50	Mean Value	Coefficient of Variation
	Subgrade Thickness (ft)	20	17	15	13	11	9	7		
Static Analysis with	Asphalt Concrete	556	375	381	412	380	441	936	497	0.38
4-inch-thick	Crushed Limestone Base	103	120	80	52	105	139	176	111	0.34
Asphalt Concrete	Subgrade	79	62	58	54	46	43	39	54	0.23
Static Analysis with	Asphalt Concrete	274	263	251	218	275	280	409	281	0.20
7-inch-thick	Crushed Limestone Base	161	221	120	106	201	308	318	205	0.38
Asphalt Concrete	Subgrade	76	65	59	57	49	46	40	56	0.20
Dynamic Analysis with	Asphalt Concrete	313	282	282	226	268	297	361	290	0.13
7-inch-thick	Crushed Limestone Base	73	68	73	79	73	76	76	74	0.04
Asphalt Concrete	Subgrade	93	88	73	79	68	65	55	74	0.17

(1) Moduli computed from the second, third, and fourth repetitions at a given load were relatively consistent and often differed from the first drop in each set of four drops. This pattern clearly supports the common practice of ignoring the first 'seating' drop.

(2) For tests at a given station, variation of backcalculated moduli was highest for the base and lowest for the subgrade (see Table 5.1).

(3) Backcalculated AC and subgrade moduli are sensitive to load level. If we delete the first drop in any series at the same load, then a sensitivity to load becomes well-defined in the remaining data. Figure 5.7 shows this pattern for the data of Table 5.1. As the load increased, the computed AC modulus increased and the computed subgrade modulus decreased.

The observations described above typify the pattern of variation found in MODULUS results for test sequences at other stations and times. In this report the moduli presented in summary tables and figures are mean values of all drops in tests sequences such as the one shown in Table 5.1.

Table 5.2 contains a summary of moduli backcalculated using MODULUS for AC thicknesses of 4 and 7 inches. Field tests for these computations occurred during morning hours with depth-averaged AC temperatures between 84°F and 89°F. Figures 5.8 to 5.10 summarize these backcalculated moduli in a plot of Young's modulus versus subgrade thickness. The abscissa for these plots is the subgrade thickness; Station Number has little physical interest as an independent variable in this case study.

Backcalculated moduli (static analysis) of the AC and base shifted to different values when the AC thickness changed from 4 to 7 inches. For the base, the average shifted upwards by 83 percent, despite a lack of change in the base's composition or thickness. The backcalculated average AC modulus decreased by 44 percent when the AC thickness changed from 4 to 7 inches. Such a change could be valid only if the added 3 inches of AC had a very low modulus. However, resilient moduli from AC cores do not support a significant difference between the two AC courses, as discussed in Chapter 7.

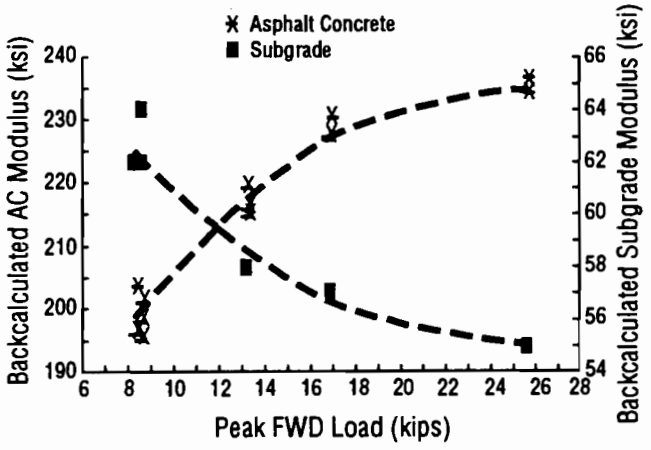

Fig 5.7. Backcalculated Young's moduli versus peak dynamic FWD load.

The modulus of the base material would not be expected to vary significantly with location and depth-to-rock. Thus, the pattern of backcalculated moduli with depth-to-rock (Fig 5.9) is difficult to explain. The wide range in statically backcalculated values may indicate that basin characteristics are relatively insensitive to base moduli in this pavement profile. The relative stability of the dynamically backcalculated results may be due in part to engineering discretion during analysis; dynamic backcalculation is not totally automated.

In Fig 5.10, all results support a trend of increasing subgrade moduli with increasing depth-to-rock. However, results from the dynamic analysis are highest—a consequence of the fact that static analyses do not account for dynamic amplification. Dynamic amplification is largest at larger radial distances. Thus, the static analysis yields lower subgrade moduli. These explanations of the difference between static and dynamic methods follow from the analytical results presented in Chapter 3.

Table 5.3 summarizes the variation of backcalculated moduli with AC temperature. Field data were obtained June 3, 1989, when the AC was 7 inches thick. Low and high AC temperatures were 87°F and 113°F, respectively. Backcalculated AC moduli plotted in Fig 5.11 clearly show the softening effect of higher temperature. The slope of the lines between points ranges from -2 to -7 ksi per degree and averages -4.2 ksi per degree Fahrenheit.

Although the AC modulus is sensitive to temperature, the limestone base and subgrade should be relatively insensitive to summertime temperature variations. Moreover, temperature changes below the AC were small. A thermocouple placed 1 inch below the surface of the base registered 94 and 98°F for low and high temperatures, respectively. The variation in subgrade temperature should be even smaller. Nevertheless, backcalculated subgrade moduli decreased by 3 to 14 percent as the AC temperature increased from the morning low to the afternoon high (Table 5.3).

LAYER MODULI FROM DYNAMIC ANALYSIS

Chapter 2 presented a brief discussion of the UTPV computer program for dynamic analysis of layered systems. The UTPV program backcalculated layer moduli for AC temperatures of 84°F to 89°F and an AC thickness of 7 inches. Moduli backcalculated for the 7-inch-thick AC worked well for the 4-inch cases with similar temperatures. For this reason, and because dynamic analyses required much computer and operator time, the

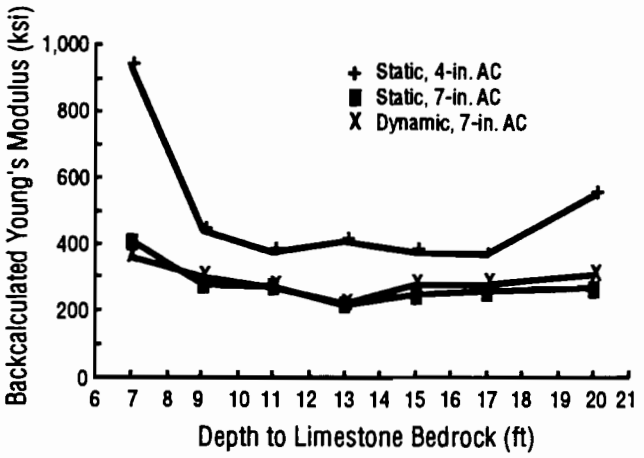

Fig 5.8. Backcalculated asphalt concrete modulus versus subgrade thicknesses.

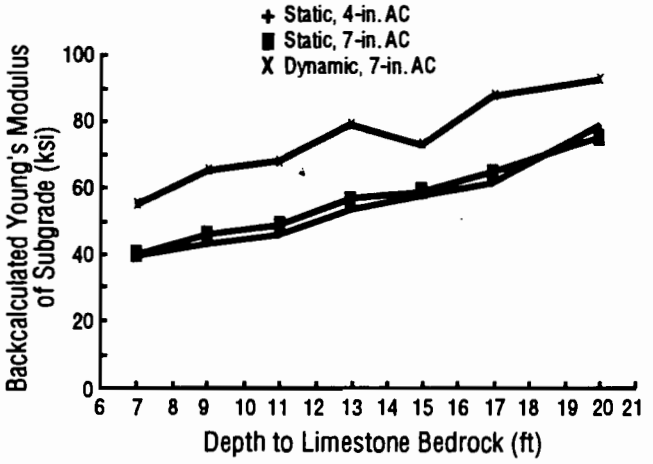

Fig 5.10. Backcalculated subgrade modulus versus subgrade thickness.

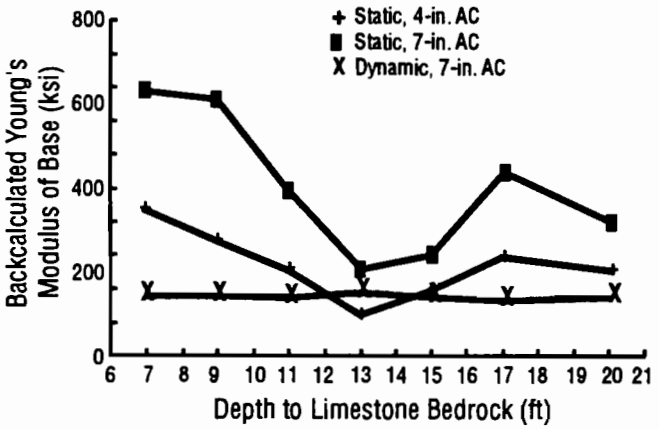

Fig 5.9. Backcalculated base moduli versus subgrade thickness.

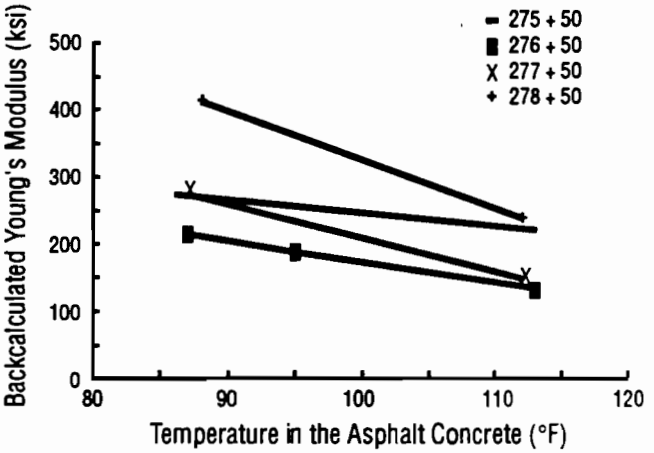

Fig 5.11. Variation of statically backcalculated modulus with asphalt concrete temperature.

TABLE 5.3. THE VARIATION OF STATICALLY BACKCALCULATED YOUNG'S MODULI (IN KSI) WITH ASPHALT CONCRETE TEMPERATURE, ASPHALT CONCRETE THICKNESS = 7 INCHES

Station Number	275 + 50	276 + 50	277 + 50	278 + 50	Mean Value	Coefficient of Variation
Subgrade Thickness (ft)	20	15	11	7		
AC Temperature (°F)	86	87	87	88	87	0.01
Asphalt Concrete	274	215	275	409	293	0.24
Crushed Limestone Base	161	120	201	318	200	0.37
Subgrade	76	59	49	40	56	0.24
AC Temperature (°F)	113	113	112	112	113	0.00
Asphalt Concrete	220	134	148	238	185	0.24
Crushed Limestone Base	135	192	110	343	195	0.46
Subgrade	73	54	43	39	52	0.25

results computed first for the 7-inch case are presented for both AC thicknesses. Table 5.2 summarizes moduli backcalculated using dynamic analysis. Figures 5.8 to 5.10 present these moduli plotted against depth-to-rock.

COMPARISON OF RESULTS FROM STATIC AND DYNAMIC ANALYSES

Figures 5.12, 5.13, and 5.14 present comparisons between measured deflection basins and computed deflection basins for depths-to-rock of 20, 15, and 7 feet, respectively. The computed basins represent deflections from static and dynamic analyses with the respective backcalculated layer moduli shown in Table 5.2. Interestingly, both methods of analysis yield computed basins which closely match the field measurements. However, moduli from the dynamic analysis may differ greatly from moduli computed with the static analysis. The fact that these methods give good basin fits with different moduli underscores the significance of dynamic behavior and dynamic models.

Moduli backcalculated for the AC layer are the least affected by the choice of static or dynamic analysis. Findings from Chapters 3 and 4 provide an understanding of this behavior: Deflections near the load center are most sensitive to the AC modulus and are least affected by dynamic amplification. Thus, backcalculated AC moduli are least affected by dynamic behavior. Conversely, deflections far from the load center can be subjected to large dynamic amplification, and these deflections significantly influence backcalculated subgrade moduli. Thus, backcalculated subgrade moduli are largest with dynamic analysis.

Figures 5.12 through 5.14 show computed reflection ratios versus distance from the load center. The reflection ratio is the ratio of deflections computed with a dynamic analysis to deflections computed for a static analysis using a static load equal to the peak dynamic load. The UTPV program was used to compute the dynamic deflections. Amplification ratios increased with distance from the load. Dynamic amplification is largest for sensors that have the largest effect on backcalculated subgrade moduli. Thus, basin fitting with static analysis requires a softened system (lower subgrade moduli) to match the measured dynamic basin. Dynamic amplification ratios explain why subgrade moduli are lowest with static analysis and why static and dynamic analyses yield similar AC moduli.

CHAPTER SUMMARY

This chapter presented results from FWD data collected on the centerline of Embankment SW with variable depth-to-bedrock, two AC thicknesses, and varied AC temperatures.

Deflections for sequential drops at a given load were relatively consistent after the initial seating load. Deflections under the initial seating load differed from subsequent deflections in a random manner. Moduli backcalculated from the initial drop also differed

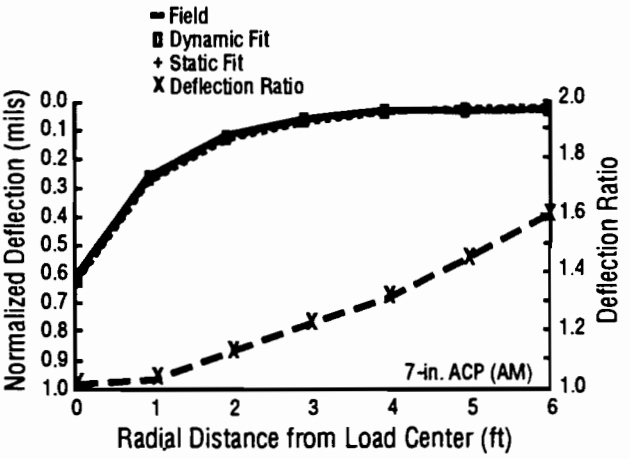

Fig 5.13. Measured and computed deflection basins for Station 276+50.

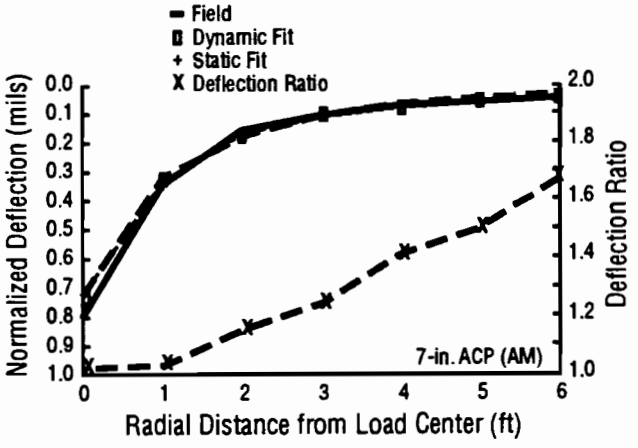

Fig 5.12. Measured and computed deflection basins for Station 275+50.

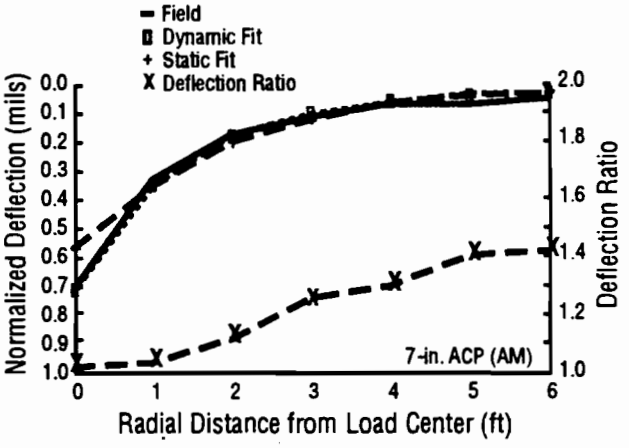

Fig 5.14. Measured and computed deflection basins for Station 278+50.

randomly from the results of subsequent drops at the same load level.

For a given load level, backcalculated subgrade moduli were relatively consistent for different drops. However, both the base and the AC moduli were variable. For a typical series of 28 drops at various loads, the coefficients of variation for the AC, base, and subgrade were 0.07, 0.12, and 0.05, respectively.

Within the static backcalculation results, the subgrade modulus clearly increased slightly as the load level increased. Conversely, backcalculated AC moduli decreased slightly as load increased. When the thickness of the AC was increased from 4 to 7 inches, the computed subgrade modulus changed little. However, the computed modulus of the AC decreased and the computed base modulus increased dramatically as the AC thickness changed from 4 to 7 inches.

The softening effect of increased AC temperature was evident in the backcalculated AC moduli. Using the average of the results for four sites, the AC modulus decreased by 4.2 ksi per degree Fahrenheit.

AC moduli obtained from static and dynamic backcalculation methods were similar. However, dynamic analysis gave significantly higher subgrade moduli. This difference between dynamic and static results was attributed to dynamic amplification of surface deflections. At a distance of 6 feet from the load, the computed ratio of dynamic and static deflections was as high as 1.6. Deflections at larger radial distances controlled the computed subgrade moduli. Thus, proper dynamic analysis yielded a stiffer subgrade.

CHAPTER 6. SPECTRAL-ANALYSIS-OF-SURFACE-WAVES TEST

INTRODUCTION

The Spectral-Analysis-of-Surface-Waves (SASW) test is an engineering seismic method that provides information about the thicknesses and moduli of layers in pavement systems. The SASW test, conducted on Embankment SW as part of this research, is a non-destructive surface test well-suited for the evaluation of pavement systems. This chapter provides general information about SASW testing, while Chapter 7 presents the specific results of SASW tests on Embankment SW. References 16, 17, and 18 contain additional and detailed information regarding SASW testing.

OVERVIEW OF THE SASW METHOD

An understanding of surface wave motion and surface wave dispersion in a layered profile is essential to understanding the SASW method. Surface waves cause individual particles on the surface to oscillate in a retrograde ellipse. However, the amplitude of motion at depth depends on the surface amplitude and the ratio of the depth to the wavelength of the surface wave. Figure 6.1 is a simplified illustration of how the amplitude of particle motion varies with depth and wavelength. The longer wavelength, λ_2, causes significant motion at greater depth than λ_1 does.

For a given wavelength, the velocity of propagation depends primarily upon the properties of the material in which significant particle motion is generated. A short wavelength concentrates particle motion near the surface and thus propagates with a velocity that indicates the properties of material close to the surface. A longer wavelength causes particle motion in deeper material and thus "samples" the elastic properties of that deeper material.

The variation of surface wave propagation velocity with wavelength (or frequency) is called dispersion. If an elastic medium's properties do not vary with depth, then all wavelengths propagate at the same velocity. Thus, in a uniform medium there is no dispersion of surface waves. In a layered system (such as a pavement structure), dispersion provides information about vertical variations of elastic properties.

The propagation velocity of a surface wave with a specific wavelength may also be called phase velocity. Measurement of phase velocities for a wide frequency (or wavelength) range provides information about material properties over an associated range of depths. Dispersion

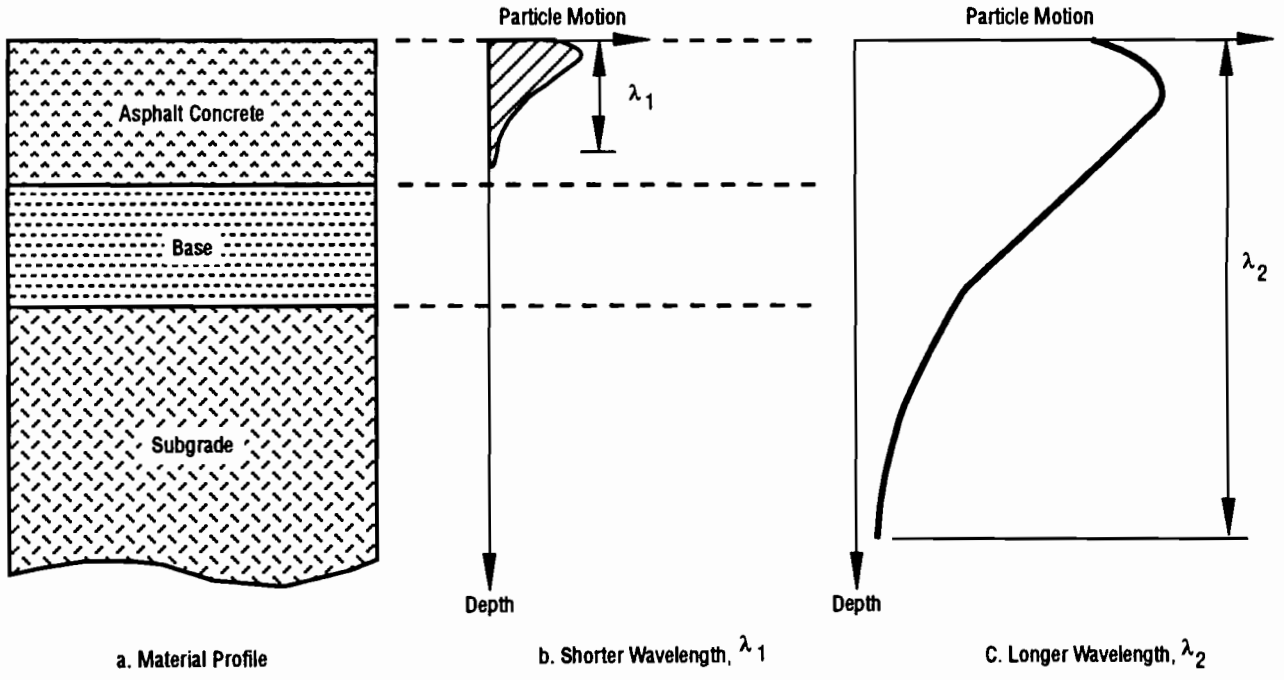

Fig 6.1. Approximate distribution of vertical particle motion with depth for two surface waves of different wavelengths (from Ref 18).

data are often presented in terms of a dispersion curve, depicting phase velocity versus wavelength, as in Fig 6.2. Dispersion curves summarize the raw field data and are the basis for computing the moduli and thicknesses of each layer in a profile.

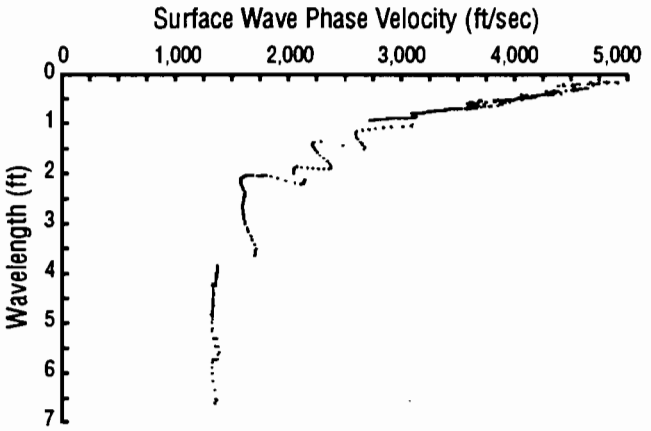

Fig 6.2. SASW dispersion curve; Station 276+50 with 7 inches of asphalt at 87°F.

In practice, the objectives of SASW field testing are to excite surface waves, measure surface motion, and record the measurements in the frequency domain. Usually, the objectives of SASW analysis are to prepare dispersion curves and then to determine the shear wave velocity and thickness of layers in the profile. The analytical procedure for computing the shear wave velocity and thickness of layers is called inversion. In current practice, inversion is an iterative matching procedure that is somewhat analogous to conventional basin fitting as discussed in Chapter 2.

An engineer performing an inversion starts with a trial profile of layers and properties and computes a theoretical dispersion curve for comparison with the measured dispersion curve. Successive adjustments to the trial profile improve the match between the computed and measured dispersion curves. The trial profile that yields a satisfactory match becomes the computed profile of shear wave velocities and layer thicknesses. Thus, as with FWD data, the results of an SASW test of a layered system are backcalculated rather than directly computed. Strictly speaking, backcalculation is not a true inversion but is a forward modeling process. In addition, the number of layers used in the SASW backcalculation process ranges from five to ten for a typical pavement profile in which stiffness is evaluated to a depth of about 10 feet.

The shear wave velocity and moduli of the top layer are often determined in the field without dispersion curves or inversion. This simplification is possible because the phase velocity of short wavelengths directly relates to the shear wave velocity in the top layer. During some analyses of data from Embankment SW, only the top layer (the AC) was of interest. In such cases the transition from surface wave phase velocity, V_r, to shear wave velocity used the following relation:

$$V_S = CV_r \tag{6.1}$$

where C is a constant that is slightly larger than unity and depends on Poisson's ratio, n. Poisson's ratio is usually estimated as it is in basin fitting for FWD data. Simple relationships from the theory of elasticity convert V_S to shear modulus, G, and Young's modulus, E:

$$G = \rho V_S^2 \tag{6.2}$$

$$E = 2G(1+\nu) \tag{6.3}$$

where ρ is mass density. Relations 6.2 and 6.3 are also used to convert the results from inversion of SASW results to the final shear and Young's moduli of various layers.

FIELD EQUIPMENT AND PROCEDURES

Procedures for rapid execution of SASW field work were developed in the Soil Dynamics Laboratory of The University of Texas. Figure 6.3 depicts the basic equipment and general configuration of the source, receivers, and recording equipment used for tests on Embankment SW.

SASW tests on Embankment SW employed hand-held hammers, electro-mechanical vibrators, and piezoelectric transducers as sources for surface waves. The choice of an appropriate source depends primarily on the wavelength requirements of a test. Short wavelengths and high frequencies sample shallow material, while long wavelengths sample deeper material. Hand-held hammers were appropriate for nearly all wavelengths except the shortest wavelengths required for profiling the upper AC layer. Electro-mechanical vibrators worked well for the medium wavelengths used to test the subgrade. Piezoelectric transducers were very effective as sources of the high-frequency waves (10 to 25 kHz) required to test the upper AC layer.

Velocity transducers (geophones) and piezoelectric accelerometers measured the surface motions caused by the wave sources. Geophones were appropriate for tests with frequencies that sampled the subgrade or any material deeper than 8 feet. Tests of the AC, base, or the upper 8 feet of the subgrade were made with accelerometers. The spacing between the source and the receiver closest to it was usually equal to the spacing between the two receivers (Fig 6.3); hence d_2=2d. Receiver spacing ranged from 0.25 to 16 feet, but most data were collected with spacings of 0.5, 1, 2, and 4 feet. Tests of the AC layer were conducted with high frequencies and receivers spaced 0.25 and 0.5 feet apart.

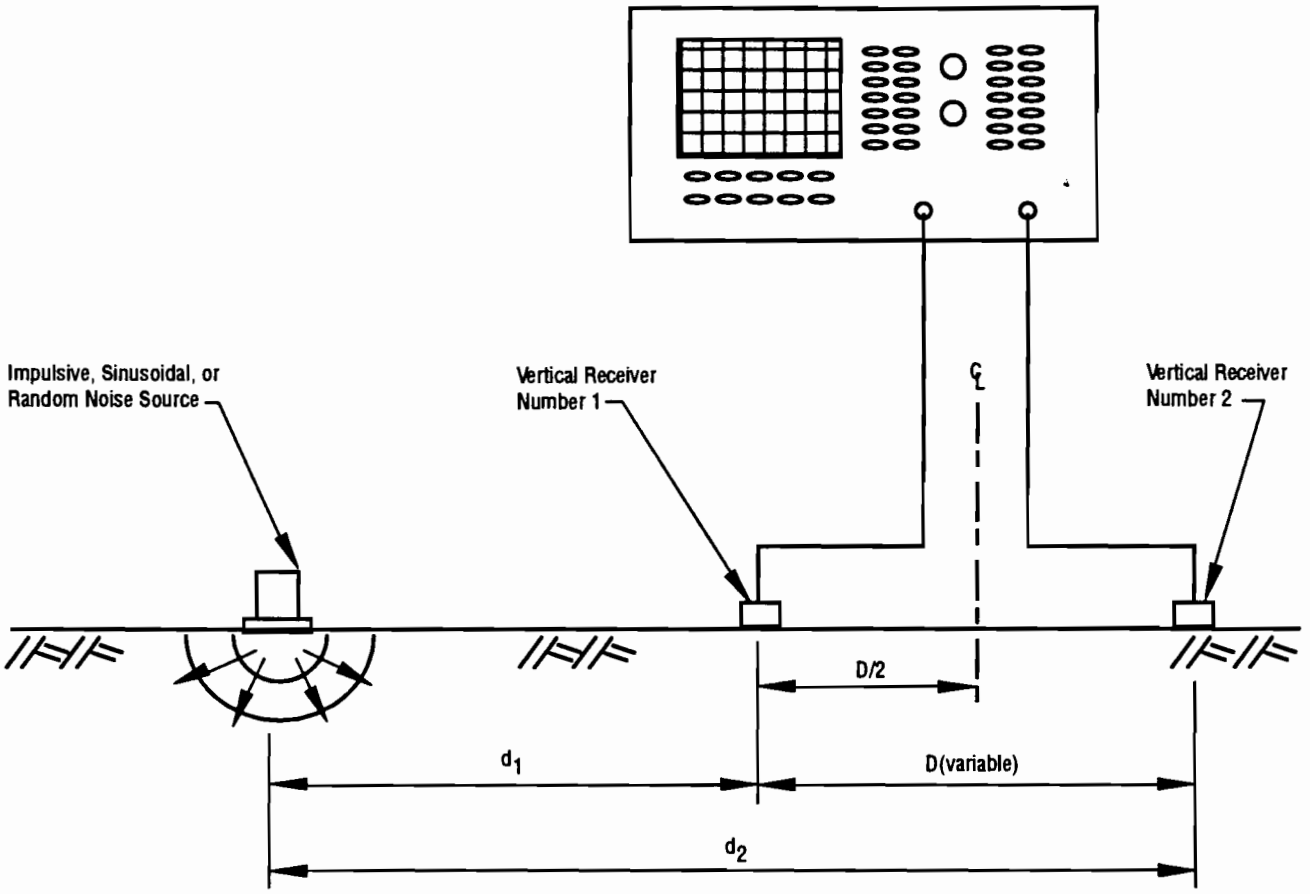

Fig 6.3. General configuration of equipment used in SASW field testing.

A dual-channel Fast Fourier Transform (FFT) analyzer recorded and processed the output from the geophones and accelerometers. For each test multiple measurements were averaged in the frequency domain and viewed by the operator. The capabilities of the FFT analyzer permitted an experienced operator to evaluate the quality and usefulness of each data set during testing. The analyzer also gave data from which the operator could make preliminary estimates of the shear wave velocity in the top layer.

SASW tests were conducted at each of the seven stations tested with the FWD. All these stations were tested with 4 and 7 inches of AC and with morning and afternoon temperatures in the AC. Thermocouples measured temperatures in the AC layers; temperature data appear in Figs 5.1 and 5.2. At stations 275+50, 276+50, and 278+50, SASW tests were also conducted to characterize the subgrade before any AC was placed.

RESULTS FROM SASW TESTS

The primary objective of SASW testing and analysis on Embankment SW was to evaluate the variation of apparent moduli with depth-to-rock, location, AC thickness, and AC temperature. SASW tests on Embankment SW provided dispersion curves relating surface wave velocity to wavelength. These dispersion data were the basis for laboratory analysis and evaluation of shear wave velocities and moduli of individual layers.

In some cases a rigorous backcalculation procedure was used to compute layer moduli from dispersion data. For SASW tests, backcalculation (or inversion, as it is usually called) can be relatively time-consuming. Fortunately, much information about layer properties can be inferred directly from the dispersion curves without inversion.

The results presented in this chapter are based on inversions and direct analysis of dispersion curves. The vertical profile of Embankment SW was presented in Figs 1.1 and 1.2; this chapter incorporates the general profile of Embankment SW shown in those earlier figures. Table 6.1 summarizes the values of Poisson's ratio and unit weight that were used for analysis of the SASW data. (NOTE: The values used for SASW analysis were based on analysis of available shear and compressional wave velocities, as well as on the judgment of the investigators. The difference between the FWD and SASW val-

TABLE 6.1. SUMMARY OF UNIT WEIGHTS AND POISSON'S RATIOS; EMBANKMENT SW

	FWD Analysis	SASW Analysis	
	Poisson's Ratio	Poisson's Ratio	Unit Weight PCF
Asphalt Concrete	0.25	0.27	145
Base	0.30	0.30	135
Fill	0.35	0.33	130

TABLE 6.2. SASW RESULTS FOR THE ASPHALT CONCRETE, EMBANKMENT SW, AUSTIN, TEXAS

		4-in. ACP				7-in. ACP			
Station Number	Depth to Rock (ft)	Frequency Range (kHz)	Surface Temperature (°F)	Phase Velocity (ft/sec)	Young's Modulus (ksi)	Frequency Range (kHz)	Surface Temperature (°F)	Phase Velocity (ft/sec)	Young's Modulus (ksi)
275 + 50	20	12 - 22	76	4,500	1,946	7-24	85	4,400	1,861
276 + 00	17	12 - 23	76	4,500	1,946	7-30	85	4,500	1,946
276 + 50	15	13 - 24	77	4,900	2,308	6-29	83	4,500	1,946
277 + 00	13	15 - 25	77	5,000	2,403	8-27	83	4,800	2,214
277 + 50	11	14 - 23	78	4,800	2,214	7-36	84	4,650	2,078
278 + 00	9	12 - 19	77	4,000	1,538	7-23	84	4,500	1,946
278 + 50	7	14 - 25	82	5,000	2,403	7-24	88	4,400	1,861
Average			77	4,671	2,108		85	4,536	1,979
Coefficient of Variation			0.01	0.07	0.14		0.02	0.03	0.06

ues is small and would, therefore, be expected to have a negligible effect on computed layer moduli.)

VARIATION OF APPARENT AC MODULI WITH DEPTH TO ROCK

Table 6.2 presents Young's moduli values for the ACP computed directly from the field dispersion curves using Eqs 6.1 to 6.3. Results are given for tests when the AC thickness was 4 and 7 inches at each station.

Because the SASW test for AC moduli sampled only the upper 2 to 6 inches of material, the rock depth does not affect the accuracy of the measurements. Roesset and others (Ref 19) have shown the significance of frequency effects on AC moduli. Moreover, because the excitation frequency in SASW testing of AC is high, frequency adjustments must be applied to the SASW data. These adjustments are discussed in Chapters 7 and 8.

VARIATION OF APPARENT AC MODULI WITH AC THICKNESS

For tests with 4 inches of AC, the average and coefficient of variation of Young's modulus were 2,108 and 0.14, respectively. After the AC thickness increased to 7 inches the average and coefficient of variation of Young's modulus were 1,979 and 0.06, respectively.

The difference between the average values is quite small and may be due in part to the temperatures recorded during the tests. The higher value of Young's modulus is associated with a lower average surface temperature. Nevertheless, computed values of students' t statistics suggest that there is little statistical basis for concluding that moduli of the final 3 inches of AC were substantially different from those of the first 4 inches at the time of testing.

COMPUTED YOUNG'S MODULUS FOR THE BASE AND SUBGRADE

Table 6.3 presents computed Young's moduli for the Base and Fill material of Embankment SW. These values (based on tests conducted June 3, 1989, when the AC thickness was 7 inches) were computed by inversion of the dispersion data. Because of the substantial effort required for each complete inversion, only the three tabulated stations were analyzed. These results are discussed in Chapter 7, where overall comparisons are made.

CHAPTER SUMMARY

SASW tests conducted near the centerline of Embankment SW provide information about Young's moduli of the AC, base, and subgrade layer. Tests were made with 4- and 7-inch thicknesses, varied AC temperatures, and varied subgrade thicknesses. Analysis of the SASW measurements is based on surface wave dispersion in a layered profile. Like basin fitting with FWA data, SASW inversion yields layer moduli from iterative forward modeling. Tables 6.2 and 6.3 present the resulting SASW data. These data are discussed in Chapter 8 using additional material presented in Chapter 7.

TABLE 6.3. SASW RESULTS FOR THE BASE AND FILL, EMBANKMENT SW, AUSTIN, TEXAS, JUNE 3, 1989

		Base		Fill		
Station Number	Depth to Rock (ft)	Phase Velocity (ft/sec)	Young's Modulus (ksi)	Phase Velocity (ft/sec)	Shear Wave Velocity (ft/sec)	Young's Modulus (ksi)
275 + 50	20	1,400	180	1,100	1,210	114
276 + 50	15	1,400	180	1,050	1,155	104
278 + 50	7	1,350	167	1,060	1,165	106

CHAPTER 7. SUPPLEMENTAL DATA FROM FIELD AND LABORATORY TESTS, EMBANKMENT SW

INTRODUCTION

FWD and SASW tests on Embankment SW were supplemented with other field and laboratory tests characterizing the material properties of the profile. Results from these tests allow a more complete evaluation of the FWD and SASW data in this case study. The following sections present the results of the supplemental tests.

SEISMIC REFRACTION SURVEY

The soil profile shown in Fig 1.2 indicates that fill material and natural soil beneath Embankment SW were underlain by limestone bedrock. Soil borings made by the Texas SDHPT and The University of Texas indicated that the surface of the intact bedrock was nearly horizontal over a relatively wide area beneath Embankment SW. In interpreting these boring logs, the surface of the intact rock was identified by drillability with standard truck-mounted drilling equipment and by rock cores. To verify the depth-to-rock, two surface seismic refraction surveys were conducted.

Both refraction surveys were made on the north side of Embankment SW such that the array of data points was parallel to the ramp and offset approximately 40 feet from the center of the 25-foot wide ramp. The stationing and positioning of each survey were arranged to minimize reflections or refractions from the ramp's retaining wall and buried drainage structures.

The first survey was conducted between Stations 274+50 and 275+00. Figure 7.1 presents the travel time data for the northbound and southbound profiles of the first survey. This travel time data allowed computation of the depth-to-rock using the methods presented by Richart, Hall, and Woods (Ref 20). The computed depth-to-rock was 6.4 feet, placing the rock at elevation 745 ft. A refraction survey between Stations 278+00 and 278+50 identified rock 8.7 feet below the surface, placing rock at elevation 747 ft (Fig 7.2).

The rock elevations determined by the seismic reflection surveys are in close agreement with data from drilling logs. These methods of investigation indicated that the rock surface elevation decreases slightly as Station Number decreases. However, this slight inclination is not sufficient to require that the rock surface be treated as an inclined layer in the analyses made for this report.

The refraction data and drillability observations actually indicate the depth at which a marked change in material stiffness occurs. Thus, it is possible that rock depths in this report coincide with the surface of the residual zone, where the transition between soil and rock begins. However, for static analysis and generally for the dynamic analysis of FWD data, the depth at which a marked material stiffness contrast occurs is the depth of interest for defining layers and for establishing the practical location of infinitely stiff bedrock.

The magnitude of the stiffness contrast between layers is clearly indicated in the plotted refraction data, since stiffness is inversely related to the square of the slope of the travel time curves. Table 7.A presents the wave velocities and layer thickness computed from the refraction survey data. Thus, near the depths discussed above, the computed material stiffnesses increased by factors of 23 to 47. It is probable that such stiffness contrasts warrant the assumption that the lower layer is infinitely stiff, provided static layer theory is used and the depth to the

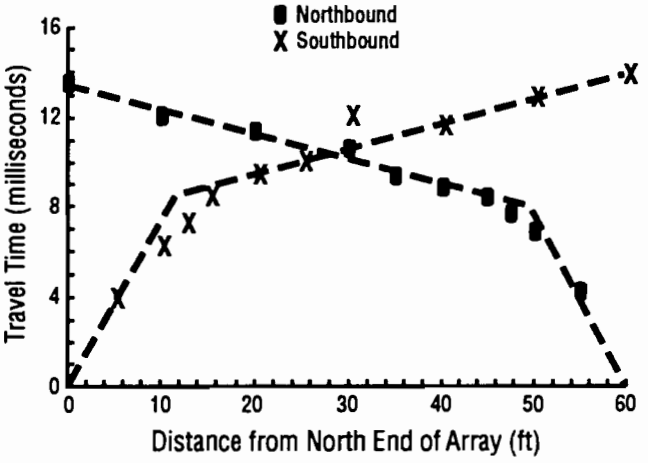

Fig 7.1. Wave travel-times from a seismic refraction survey, Stations 274+50 to 275+00.

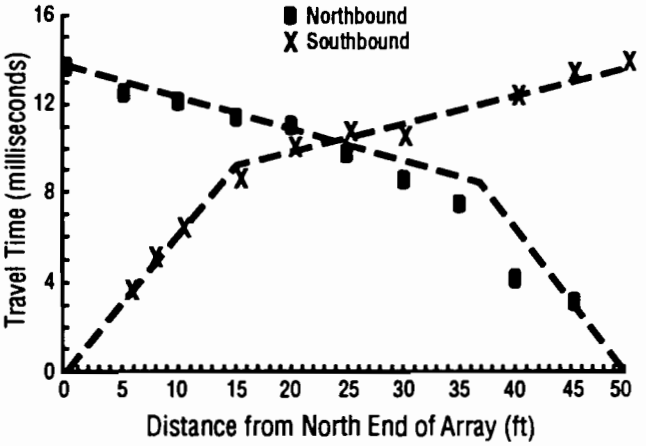

Fig 7.2. Wave travel-times from a seismic refraction survey, Stations 278+00 to 278+50.

lower layer is sufficiently large relative to the thickness of the asphalt concrete pavement.

CROSSHOLE SEISMIC TESTS

Crosshole seismic tests were conducted at Stations 275+50, 276+50, and 278+50. At each test location two boreholes were drilled 5 feet apart on the centerline of the ramp. Station 276+50 was tested to a depth of 11 feet, while Stations 275+50 and 278+50 were tested to depths of 5 feet below the base material. Tests were conducted and analyzed after the methods presented by Stokoe and Hoar (Ref 21).

The crosshole test data provided wave travel times from which the velocities of compressional waves, V_p, and shear waves, V_s, were computed. Data from crosshole wave measurements are shown in Fig 7.3, with the dashed lines representing average values. Individual values of the shear wave velocity are reported in Table 7.1. The measured values of V_s and V_p allowed calculation of Poisson's ratio, ν, from the following relation for isotropic materials:

$$\nu = \frac{v_p^2 - 2v_p^2}{2\left(v_p^2 - v_p^2\right)} \qquad (7.1)$$

The average value of Poisson's ratio for the fill was 0.33. Shear Modulus, G, and Young's modulus, E, were computed using the measured shear wave velocities, Poisson's Ratio, and mass density, ρ:

$$G = \rho\, v_s^2 \qquad (7.2)$$

$$E = 2G\,(1 + \nu) \qquad (7.3)$$

Based on thin-walled tube samples, the average unit weight of the subgrade was 130 pcf. Thus, the mass density was taken as 4.04 lbm/ft^3. For the upper 5 feet of each test, Young's moduli of 118, 105, and 73 ksi were computed for Stations 275+50, 276+50, and 278+50, respectively. The average velocity for Station 276+50 with depth between 2 and 11 feet yielded a slightly higher Young's modulus of 113 ksi. The depths-to-bedrock for Stations 275+50, 276+50, and 278+50 were taken as 20, 15, and 7 feet, respectively.

TABLE 7.A. REFRACTION SURVEY RESULTS; SURVEY LINE PARALLEL TO RAMP SW AND OFFSET APPROXIMATELY 40 FEET WEST OF THE RAMP CENTERLINE

Test	Depth (ft)	P-Wave Velocity (ft/s)
Station 274+50 to 275+00	0 to 6.4	1320
	> 6.4	9060
Station 278+00 to 278+50	0 to 8.7	1606
	> 8.7	>640

RESONANT COLUMN TESTS OF THE SUBGRADE

Torsional resonant column (RC) tests were made with subgrade specimens carved from 3-inch-diameter tube samples of the fill. The resonant column test is based on theoretical solutions which relate the stiffness or modulus of a soil column to its resonant frequency (Refs 20 and 22).

All testing was conducted with torsional excitation using equipment in the Soil Dynamics Laboratory of The University of Texas at Austin. The subgrade specimens were tested to evaluate shear modulus, G, over a wide range of confining pressures, σ_0, and shear strain amplitudes, γ. Young's modulus, E, was computed using Eq 7.3, and the equivalent axial compressional strain, ε, was computed from the shear strain and Poisson's ratio as follows:

$$\varepsilon = \gamma / (1 + \nu) \qquad (7.4)$$

The results shown in Fig 7.4 were for a sample depth of 7 feet at Station 276+50. At a given confining pressure the highest modulus, E_{max}, occurs at the lowest strain. For equivalent axial strain less than a threshold of about 0.001 percent, the computed Young's modulus is independent of strain and is close to E_{max}. As strain increases above the threshold strain, the modulus becomes markedly dependent on strain level. Moduli from resonant column tests should be close to effective secant moduli at the respective strain levels.

An alternate presentation of the non-linear load deformation behavior of these soils is shown in Fig 7.5. In this figure the modulus is divided by the initial tangent modulus, E_{max}, and again plotted against strain. The nonlinear behavior shown in Fig 7.5 is typical of many soils. From these data it is clear that the effective stiffness at points in even a uniform subgrade will depend upon the strain level.

Peak principle strain levels in a hypothetical pavement profile were calculated using the ELSYM5 program (Ref 4) and appear in Fig 7.6. The pavement profile consisted of 4 inches of AC, 6 inches of base, and 15 feet of subgrade over rock. Strains were computed for points directly beneath a 10 kip wheel-load with an area of 190 square inches (FWD load pad). Young's moduli for the AC, base, and subgrade were 350, 110, and 60 ksi, respectively. These modulus values were selected based on anticipated ranges for these layers.

The computed principle strain values suggest that subgrade material within several feet of the base may be loaded to strains well over the 0.001 percent strain threshold. Only when a depth of approximately 60 inches is obtained are the strains close to the threshold value. In view of these data, and recognizing that strain

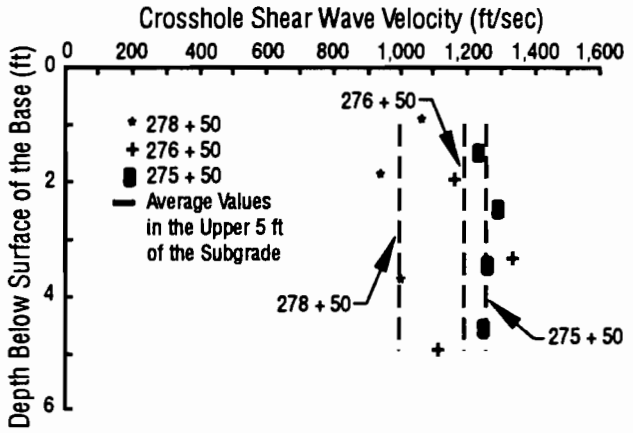

Fig 7.3. Wave velocities measured by crosshole method in the subgrade.

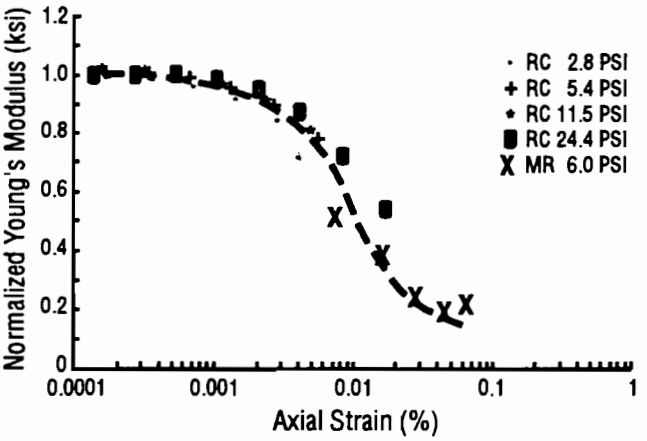

Fig 7.5. Normalized Young's modulus versus axial strain, subgrade at Station 276+50.

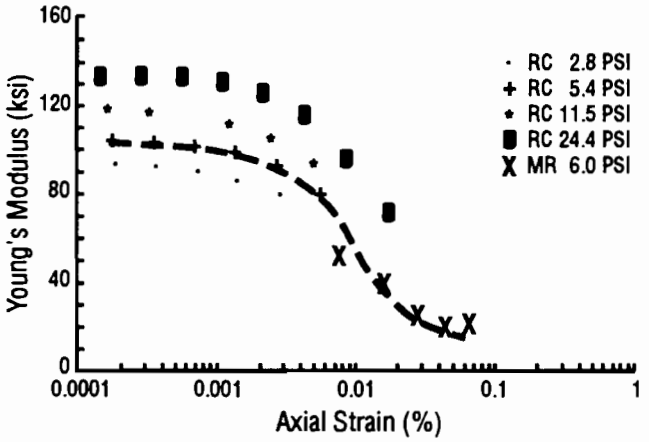

Fig 7.4. Variation of subgrade stiffness with axial strain amplitude and confining pressure as determined by resonant column and resilient modulus tests, Station 276+50.

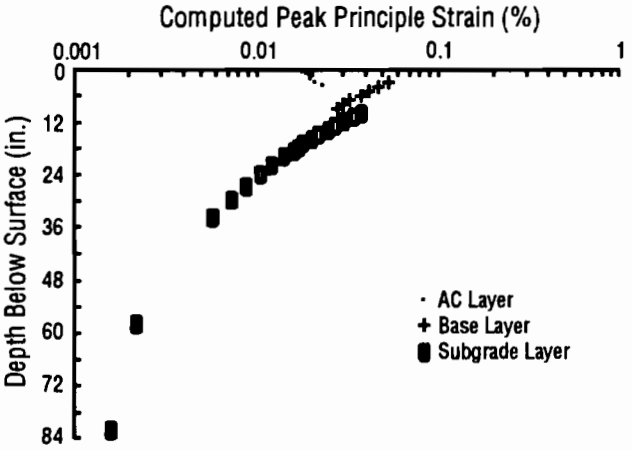

Fig 7.6. Peak principal strains computed with ELSYM5 for a static 10 kip wheel load.

TABLE 7.1. CROSSHOLE SEISMIC MEASUREMENTS, EMBANKMENT SW

Station 278 + 50			Station 276 + 50			Station 275 + 50		
Depth (ft)	S-Wave (ft/sec)	P-Wave (ft/sec)	Depth (ft)	S-Wave (ft/sec)	P-Wave (ft/sec)	Depth (ft)	S-Wave (ft/sec)	P-Wave (ft/sec)
1	1,050	1,930	2	1,150	2,470	1.5	1,230	2,610
2	930	1,940	3.42	1,320	2,810	2.5	1,290	2,230
4	990	2,370	5	1,100	2,130	3.5	1.260	2,350
			7	1,500	3,200	4.6	1,250	2,350
			9	1,300	2,590			
			10	1,210	2,190			
			11	1,030	2,230			
Avg[1]	990	2,080		1,190	2,470		1,258	2,385

[1]Averaged over the upper 5 feet.

also varies laterally away from the load, it is clear that a single correct modulus cannot be defined for typical subgrades and profiles. Rather, the modulus changes with confining pressure (depth) and with strain level.

RESILIENT MODULUS TESTS OF THE SUBGRADE

One soil specimen from a depth of 7 feet at Station 276+50 was tested according to the revised AASHTO resilient modulus test for soils (Ref 23). The confining pressure for this test was 6.0 ksi; the results are plotted with resonant column data in Fig 7.4. The plotted data were all measured on a single sample used for both tests. The measured resilient modulus values, M_R, follow the same pattern of strain magnitude dependency as do the resonant column data.

RESONANT COLUMN TESTS OF THE ASPHALT CONCRETE

Resonant column tests were made with a 2-inch-diameter sample of AC cored from Embankment SW at Station 276+50. A series of unconfined RC tests were conducted in a thermal bath with controlled variable temperatures. The AC temperatures ranged from 73°F to 119°F. Results from this series of tests are presented in Fig 7.7. The moduli are relatively independent of strain up to and beyond 0.001 percent axial strain. Because the testing apparatus was designed for load levels associated only with typical soil samples, strains beyond approximately 0.003 percent were not achieved.

The significance of AC temperature appears clearly in Fig 7.3. The modulus at 73°F was approximately 3.3 times higher than the value at 119°F. This temperature range is similar to that measured during field tests on Embankment SW.

RESILIENT MODULUS TESTS OF THE ASPHALT CONCRETE

The Pavement Research Laboratory of The University of Texas performed Resilient Modulus tests and Indirect Tensile Tests on twelve 4-inch-diameter asphalt concrete-cored specimens. These cores were taken from Stations 275+50, 276+50, and 278+50 after the AC thickness reached 7 inches. The temperature of the AC cores was 77°F during testing. Separate tests were made for material from the 4-inch and 3-inch-thick layers. Table 7.2 presents the results from these tests. Averaging the results from each station provided M_R values of 623, 445, and 609 ksi for Stations 275+50, 276+50, and 278+50, respectively.

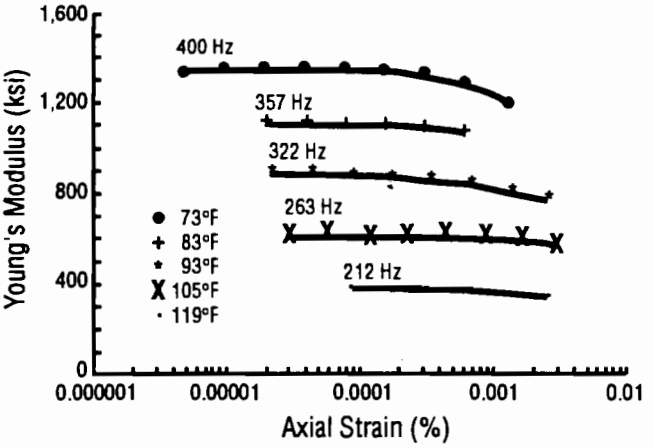

Fig 7.7. Variation of Young's modulus with asphalt temperature and axial strain, Embankment SW.

CHAPTER SUMMARY

This chapter presented reference data from supplemental field and laboratory tests. Results from the seismic refraction survey assisted in a definition of the elevation of the surface of the intact rock. This was used to confirm the approximate thicknesses of the subgrade (see Fig 1.1 and Table 5.2).

The crosshole results provide additional information about the stiffness of the subgrade at seismic level shear strains on the order of .001 percent. Young's moduli from these low strain tests ranged from 73 to 118 ksi.

Torsional resonant column (RC) tests of subgrade samples from a depth of 7 feet at Station 276+50 provided information about Young's modulus as a function of axial strain. Strains in the RC tests ranged from .0002 to .02 percent. This range of strains overlaps the data from resilient modulus tests on a sample from the same depth and station. Taken together (Figs 7.4 and 7.5), these data illustrate the dependence of modulus on strain. These data are also suitable for critical comparison with appropriate data from SASW and FWD tests.

Asphalt concrete cored from Embankment SW was tested in the resonant column device and in asphalt resilient modulus tests. These data provide values and trends of asphalt modulus as a function of strain and temperature. The measured temperature effects will be utilized in Chapter 8, which provides a synthesis of the available data.

TABLE 7.2. SUMMARY OF INDIRECT TENSILE AND RESILIENT MODULUS TESTS ON ASPHALT CONCRETE CORES, EMBANKMENT SW

Station Number	Sample Number	Air Voids (%)	Indirect Tensile Strength (psi)	Resilient Modulus (ksi)
275 + 50	T-3	6.28	87	643
275 + 50	T-4	4.99	100	616
275 + 50	B-3	4.73	100	627
275 + 50	B-4	4.50	109	605
	Average:	5.12	99	623
276 + 50	T-1	7.42	78	374
276 + 50	T-2	7.64	77	348
276 + 50	B-1	4.63	136	441
276 + 50	B-2	4.87	103	618
	Average:	6.14	99	446
278 + 50	T-5	5.94	86	425
278 + 50	T-6	5.48	88	613
278 + 50	B-5	4.65	124	550
278 + 50	B-6	5.22	97	849
	Average:	5.32	99	609

CHAPTER 8. COMPARISON AND EVALUATION OF APPARENT MODULI FROM FWD AND SASW MODELS

INTRODUCTION

The data and analyses from research on Embankment SW allow comparison of results obtained with the FWD and SASW methods. Moreover, the results can be evaluated against data from supplemental tests conducted in the field and in the laboratory. This chapter compares and evaluates the available data for the subgrade and asphalt concrete (AC) of Embankment SW. (This case study generated insufficient data to consider the 6-inch-thick base layer; it is therefore not discussed.)

YOUNG'S MODULUS OF THE SUBGRADE

Results from all tests of Embankment SW subgrade material are summarized in Fig 8.1. FWD results are the average of tests with 4 and 7 inches of AC. Results from resonant column (RC) and resilient modulus (M_R) tests are for average effective confining pressures of 5.4 and 6.0 psi, respectively. These confining pressures are appropriate for a depth of approximately 7 feet.

All field test data (FWD, SASW, and crosshole) indicate that, moving up the embankment, subgrade stiffness increases. This common trend strongly suggests that actual in-situ stiffness increases with increasing depth of fill. The parallel results also suggest that each method was sensitive to lateral variations in the subgrade material stiffness. It is possible that changes in compactive effort caused this trend of in-situ stiffness on Embankment SW. The overall averages for subgrade moduli computed from FWD using static and dynamic analyses are 55 and 74 ksi, respectively (Table 5.2). The difference between FWD results from static and dynamic back-calculation (basin-fitting) methods (Fig 8.1) is attributed to dynamic amplification. Figures 5.12 to 5.14 presented the relation between deflections due to static and dynamic analyses of FWD loads at three stations on Embankment SW. Two or more feet from the load center, computed deflections were significantly larger for the dynamic load than for the static load. To match these dynamically amplified deflections, static basin-fitting must use a softened subgrade.

STRAIN MAGNITUDE EFFECTS IN THE SUBGRADE

Data from FWD, RC, and M_R tests indicate that results are sensitive to strain magnitude. The tendency of the modulus to decrease with strain for strains above 0.001 percent in RC and M_R tests is clearly seen in data presented in Figs 7.4 and 7.5. Within FWD data, backcalculated Young's moduli of the subgrade decreased by approximately 10 percent as the load increased from 8 to 16 kips. This apparent strain sensitivity in FWD data is presented in Fig 5.7.

In this report most analyses of FWD data used deflection basins measured under peak loads of 8 to 13 kips. Static analysis of Embankment SW suggested that a load of 10 kips will cause strains of approximately 0.04 percent near the top of the subgrade and 0.002 percent at a 6-foot depth. For such a load the effective secant modulus of soil elements will increase with depth, as strain decreases with depth. The backcalculated value represents an effective or net modulus for a particular load level and subgrade thickness. Thus, subgrade moduli backcalculated from FWD data seem to represent the material at higher strains.

Because moduli backcalculated from FWD data represent a layer response, care must be exercised when using the value as a material property in later linear elastic pavement analysis. For example, if field tests use a load of 10 kips, then backcalculated subgrade moduli may be too high for reliable analysis of loads higher than 10 kips. If the field test and later analysis with the backcalculated moduli use similar load levels, then the practical effect of non-linear behavior is taken into account.

The differences between RC and M_R moduli for similar samples are primarily due to the strain levels achieved in the test apparatus. Axial strains in the RC tests ranged from less than 0.0001 percent to 0.054 percent. Axial strains in the M_R tests ranged from 0.007 to 0.064 percent. The above-mentioned strain ranges are

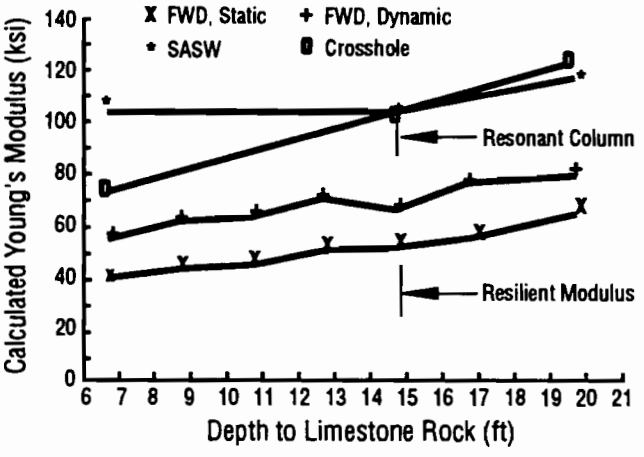

Fig 8.1. Summary of results for the subgrade, Embankment SW.

probably typical of the respective techniques used with soil samples. Figure 7.4 illustrated the continuity of the RC and M_R results corrected for strain range effects.

The strain levels associated with SASW testing on Embankment SW are less than 0.0001 percent. Thus, SASW testing measured the initial tangent moduli, E_{max}, of the layer material. For certain load levels, layer profiles, and depths the initial tangent moduli may be appropriate. For Embankment SW, E_{max} was probably appropriate for depths of 8 feet or more. However, SASW results for shallower depths in the subgrade of Embankment SW must be corrected to account for non-linear behavior.

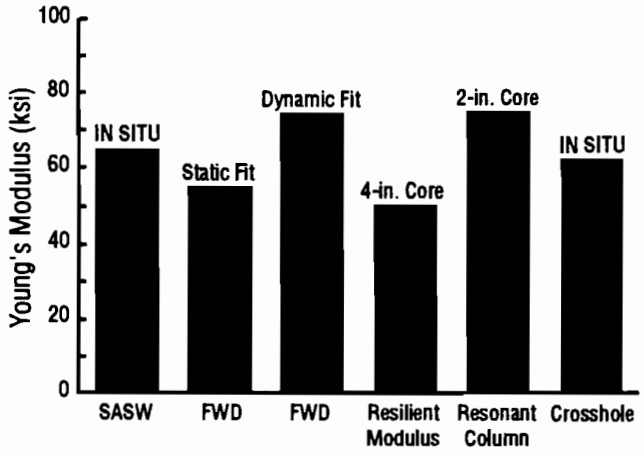

Fig 8.2. Subgrade modulus results adjusted for 0.007 percent axial strain with unadjusted FWD results, Embankment SW.

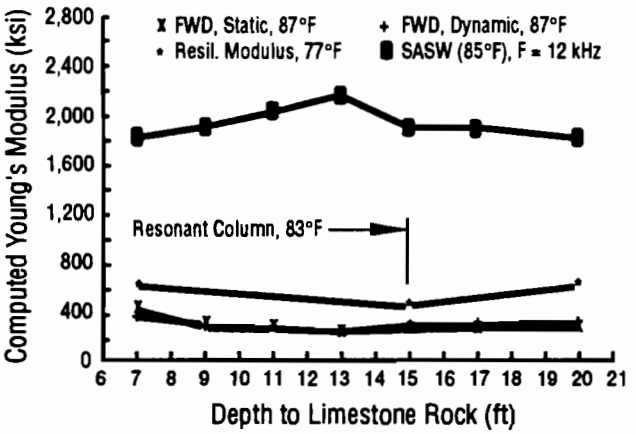

Fig 8.3. Summary of moduli for the asphalt concrete, Embankment SW (without adjustments for frequency and temperature).

ADJUSTMENTS FOR STRAIN MAGNITUDE EFFECTS IN THE SUBGRADE

Young's modulus and shear modulus of soils are typically insensitive to those strains having less than a threshold value of approximately 0.001 percent (Refs 22 and 24). For strains less than the threshold, the soil behaves linearly and moduli are at a maximum value, E_{max}. Young's modulus for strains in the non-linear range beyond the threshold strain may be normalized through division by E_{max}. For Embankment SW, a characteristic curve such as that shown in Fig 7.5 is obtained by normalization.

Seed and Idriss (Ref 25) presented curves relating shear wave velocity to shear strain for sands. Using Eqs 6.2 and 6.3, the generalized design curves presented by Seed and Idriss can be presented as Young's modulus versus axial strain. From such generalized curves the effective secant modulus for any strain could be evaluated from reliable results from another test at a known strain.

To account for the effects of strain magnitude, the pavement engineer must consider the effective strain range for a particular material test. He must also consider the strain magnitude caused by the design load. Moreover, the sensitivity of modulus to strain must be recognized when the results of different tests types are compared and applied.

Strains associated with SASW tests of pavements are always below the threshold strain where non-linear behavior begins. Because SASW tests always measure E_{max}, SASW results are readily adjusted to other strain levels. In some other tests, including the FWD, strain during the test is either uncertain or varies with depth and radius. If strain level adjustments are desired for the results of such tests, then in-situ strain during the test becomes an unknown variable that must be approximated.

TABLE 8.1. SUMMARY OF COMPUTED SUBGRADE MODULI WITH STRAIN MAGNITUDE CORRECTIONS TO 0.007 PERCENT AXIAL STRAIN

Test	Average Test Result	Judged Effective Test Strain (%)	Strain Magnitude Correction	Corrected Young's Modulus (ksi)
SASW	108	<0.0001	0.60	65
FWD, Static Fit	55	0.007	1.00	55
FWD, Dynamic Fit	74	0.007	1.00	74
Resilient Modulus	50	0.007	1.00	50
Resonant Column	103	0.0002	0.73	75
Crosshole	103	<0.0001	0.60	62

SASW, crosshole, RC, and M_R data for Embankment SW were adjusted (using the data collected in this case study) to strain levels predicted for a 10-kip FWD load. From Fig 7.6 the axial strains in the subgrade for a 10-kip FWD load vary with depth and are typically between 0.02 and 0.002 percent. The approximate effective axial strain was taken as 0.007 percent (no strain correction was made).

The relation of strain to modulus was quantified using the curves of normalized Young's modulus versus strain shown in Fig 7.5. These curves were obtained directly from laboratory RC and M_R tests. (Generalized curves such as those based on Seed and Idriss were not required.) From Fig 7.5 the effective modulus at 0.007 percent strain would be 0.5 to 0.7 of the initial tangent modulus, E_{max}. Using an adjustment factor of 0.6 with average E_{max} values from SASW, crosshole and RC tests yielded predicted Young's moduli of 65, 62, and 75 ksi, respectively.

For the M_R test the adjusted modulus of 50 ksi at 0.007-percent strain was interpolated directly from available data. Confining pressures in the M_R and RC tests were 6.0 and 5.4 psi, respectively. Figure 8.2 compares the various results adjusted to an axial strain of 0.007 percent. Table 8.1 presents a summary of these results for the subgrade.

YOUNG'S MODULUS OF THE ASPHALT CONCRETE

Computed Young's moduli for the AC layer appear in Fig 8.3. The information was obtained from static and dynamic analysis of FWD data, SASW, resonant column, and resilient modulus. The AC temperature during each test is noted in the legend of Fig 8.3.

Results from FWD testing at 87°F are the lowest values and averaged 281 and 290 ksi for static and dynamic analyses, respectively. Using Fig 7.6 as a guide, the axial strain in the AC was approximately 0.02 percent. Resilient modulus tests conducted in the pavement research laboratory at 77°F averaged 559 ksi; peak axial strain was typically 0.02 percent.

Resonant column tests conducted at temperatures of 73 to 119°F were presented in Fig 7.7. Axial strains were less than 0.003 percent. At these low strains the computed moduli were only slightly effected by strain level. For AC at 83°F the computed initial tangent modulus, E_{max}, was 1106 ksi.

SASW results for the AC appear as the upper curve in Fig 8.3. The SASW results are relatively consistent and significantly higher than the other methods. The difference between these SASW and RC results cannot be attributed to strain level because the RC tests included strains that were below the threshold strain (Fig 7.7). Because of the lack of complete data on AC strain sensitivity, strain level corrections were not applied to AC results. Although such strain magnitude corrections would be rational, they would not be as significant as strain corrections in the subgrade. This is because the variations in strains were smaller and less variable among the AC tests. Moreover, the AC test strains may be reasonably close to the AC linear range.

EXCITATION FREQUENCY EFFECTS IN THE ASPHALT CONCRETE

Roesset (Ref 26) discussed the marked effect of excitation frequency on measured Young's modulus for asphalt (his data ranged from frequencies of 0.01 Hz to 10 kHz). Chomton and Valayer (Ref 27) presented data for frequencies between 0.06 and 20 Hz. Modulus values reported by Roesset differ from those of Chomton because different materials, different apparatus, and different test

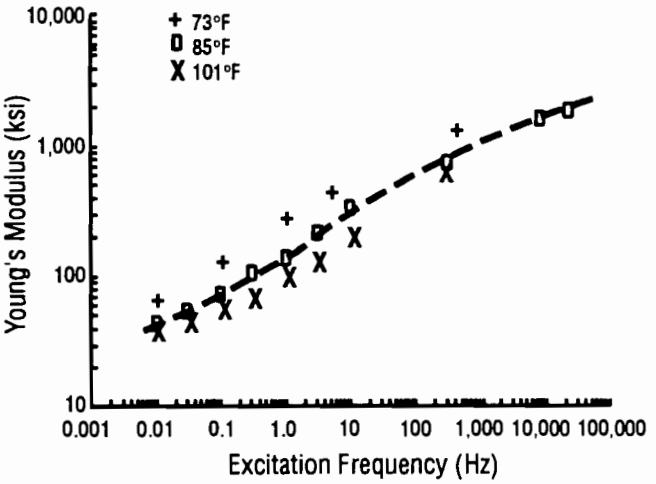

Fig 8.4. Variation of Young's modulus of asphalt concrete with excitation frequency and temperature, Embankment SW.

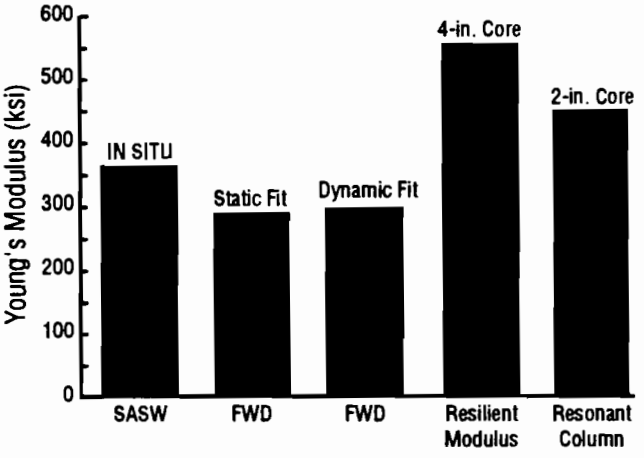

Fig 8.5. Asphalt concrete results adjusted to 20 Hz and 85∞F, Embankment SW.

temperatures were used. However, over the frequencies tested by both groups, the reported frequency sensitivity was very similar. Data presented by Roesset for samples from Embankment SW appear in Fig 8.4. For frequencies less than 100 Hz, the data were obtained from torsional shear tests. The data near 300 Hz were from RC tests, and the points above 1,000 Hz were from SASW tests in situ. The continuity between test methods is quite good.

The auto spectrum of velocity due to an FWD impact on Embankment SW was presented in Fig 2.3. FWD impact energy was concentrated between 2 and 40 Hz, with 20 Hz representing a characterizing average. SASW results for the AC at 85°F on Embankment SW may be corrected from a frequency of approximately 12 kHz to the FWD's 20 Hz using Fig 8.4. For this frequency change, the AC modulus is predicted to drop by a factor of 4.75, per Fig 8.4. The frequency-dependent correction reduced the average SASW result for 85°F from 1979 ksi to 416 ksi. This correction places the SASW results above the FWD results for 87°F and below the resilient modulus tests at 77°F.

In the RC tests at 83°F the excitation frequency was close to 350 Hz. The reduction factor between 350 and 20 Hz is approximately 2.25. Thus, RC data corrected to 20 Hz yielded a Young's modulus of 467 to 491 ksi, depending on the strain magnitude. The excitation frequency correction for the M_R test caused the M_R result to be increased by a factor of 1.28. This factor is based on the data in Fig 8.4, assuming a predominant M_R frequency of 10 Hz. Thus, the M_R result corrected for a frequency of 20 Hz was 715 ksi.

TEMPERATURE EFFECTS IN THE ASPHALT CONCRETE

The variation of AC moduli with temperature for specific excitation frequencies can be computed from the data in Fig 7.7. Expressed in relative terms, as a percentage temperature sensitivity, was highest for high temperature and low frequency (1 Hz). At 1 Hz between 85°F and 101°F Young's modulus decreased by 6.2 percent per degree Fahrenheit. At 110 Hz between 73°F and 85°F Young's modulus decreased 2.4 percent per degree Fahrenheit. However, in absolute terms temperature sensitivity was higher for high frequency and low temperature. At 110 Hz and between 73°F and 85°F the modulus decreased 23 ksi per degree Fahrenheit. At 1 Hz and between 85°F and 110°F the modulus decreased only 3.4 ksi per degree Fahrenheit.

The data presented in Fig 8.4 also quantify the effect of temperature on AC moduli. These data were used to develop frequency and temperature data corrections for AC moduli. Using data presented in Fig 8.4, AC test data for Embankment SW was adjusted first to a frequency of 20 Hz, and then to a temperature of 85°F. It was assumed that a 20-Hz excitation characterized the FWD; no frequency adjustment was applied to FWD data. Adjusted data for each method were compared in Fig 8.5. Results from FWD tests were 291 and 301 ksi for the static and dynamic basin-fitting, respectively. SASW and resonant column yielded 359 and 442 ksi, respectively. Resilient modulus tests yielded 523 ksi without a correction for frequency effects. These computed correction factors and corrected moduli appear in Table 8.2.

TABLE 8.2. SUMMARY OF COMPUTED ASPHALT CONCRETE MODULI WITH FREQUENCY AND TEMPERATURE CORRECTIONS TO 20 HZ AND 87°F

Test	Average Test Result (ksi)	Test Frequency (Hz)	Frequency Correction to 20 Hz	Test Temperature (°F)	Temperature Correction to 87°F	Corrected Young's Modulus (ksi)
SASW	1,979	12,000	.190	85	.956	359
FWD, Static Fit	281	20	1.000	87	1.000	281
FWD, Dynamic Fit	290	20	1.000	87	1.000	290
Resilient Modulus	559	10	1.27	77	.737	523
Resonant Column	1,106	350	.444	83	.901	442

CHAPTER 9. CONCLUSIONS AND RECOMMENDATIONS

The following findings and recommendations derive from this case study.

(1) Analysis based on static layer theory of a pavement profile similar to that of Embankment SW illustrated the behavior of surface deflections under static loading. The modulus of an upper 7-inch-thick AC layer heavily influenced the slope of the deflection basin within 2 feet of the load center. Deflections were insensitive to reasonable variations of the base modulus. The modulus of the subgrade affected deflections within the entire basin. However, 5 feet or more from the load center of this stiff pavement system, the surface deflections were small relative to the nominal measurement accuracy of the FWD. The thickness of the subgrade, or depth-to-rock, can have a significant effect on surface deflections. When rock is at a shallow depth, say less than 15 feet, then variations in rock depth significantly affect surface deflections, particularly for a radial distance of 4 feet or more.

(2) Dynamic analyses of the layered profile indicate that peak dynamic deflections exceed static deflections computed for the same peak load. The dynamic amplification can be very large, especially at longer distances from the load, and may increase deflections by a factor of 1.5 or more.

(3) The MODULUS computer program from the Texas Transportation Institute (Ref 7) was used for static backcalculation of layer moduli from surface deflections. This program provided very satisfactory results when used to analyze accurate computed surface deflections with known layer thicknesses. However, in the context of static backcalculation analysis, errors will occur from uncertainty in measured deflections and in-situ layer thicknesses. Significant additional error will result from neglecting the dynamic aspects of the FWD test. This error will appear greatest in the subgrade results.

(4) The UTPV (Ref 8) program provided dynamic analyses of FWD measurements. Such analyses provided valuable insight into analysis of FWD data. Both the analytical and experimental data in this case study indicate that recognition of dynamic behavior is important for proper determination of the subgrade modulus. However, although the UTPV program accounts for dynamic behavior, it requires much operator and computer time.

(5) Surface deflections measured with an FWD on Embankment SW supported the findings presented above. The field data also confirm the importance of making an initial seating drop with the FWD. For drops after a seating drop at a given load, the measured deflections and backcalculated moduli were relatively consistent. Although peak FWD loads routinely varied between 7 and 24 kips, the cause of apparent non-linearity was difficult to explain: computed subgrade moduli increased with increasing loads and AC moduli decreased with increasing loads. All FWD data were collected relatively easily and quickly with a Dynatest 9000 FWD. With only minimal training, operators were able to collect much data easily.

(6) Spectral Analysis of Surface Wave (SASW) tests provided values for the moduli of the AC and subgrade. Such results were obtainable directly from the dispersion waves for each test. Moduli of the base were obtained from detailed inversion of the dispersion data. Field measurements were generally made with a minimum of difficulty with equipment. However, aspects of the field work and analysis did require significant coordination and experience.

(7) The results from FWD and SASW tests were supplemented with results from crosshole, resonant column, resilient modulus, and cyclic torsional shear tests. These results provided a basis for calculation of the effects at differing excitation frequency, temperature, and strain in FWD and SASW tests.

(8) Subgrade moduli computed from FWD and SASW tests principally differ in that the methods induce mostly different strains in the subgrade. FWD tests generate a range of strains, but a value of 0.007 percent axial strain may characterize the overall subgrade strain. SASW tests generate strains below 0.001 percent. Because of the non-linear behavior of the soils, the tests yield different effective moduli. SASW tests provide an initial tangent moduli, while FWD gives an effective secant moduli. Based on resonant column and resilient modulus test results, SASW test results were adjusted to the strain level of the FWD. These results, presented in Fig 8.2, show the SASW subgrade moduli were between the static and dynamic FWD results.

(9) The data in Chapters 7 and 8 show the effects of both excitation frequency and temperature on the modulus of AC cores from Embankment SW. Because the excitation frequencies of SASW and FWD differ, a frequency correction is essential for comparison of results. Both these corrections were made to the AC moduli presented in Fig 8.5. The results indicate reasonable practical agreement between SASW and FWD results.

(10) The differences between results from static and dynamic analysis of FWD data can be readily predicted and understood. These differences are most significant for the subgrade layer. However, dynamic analysis is relatively difficult and time-consuming. Because of the importance of dynamic

effects, it is recommended that some level of dynamic analysis be incorporated into FWD analysis. One promising method is to develop a catalog of dynamic amplification factors for commonly encountered highway profiles. Appropriate amplification factors would then be used to adjust FWD field data prior to backcalculation. This approach is readily within current capabilities for automated data analysis.

(11) Based on the data collected in this case study, an increase in deflection measurement accuracy is recommended for the FWD—especially for the geophones spaced more than 3 feet from the load center. This quality control measure is most appropriate for FWD units used to test relatively stiff pavement profiles, such as those found on Embankment SW.

REFERENCES

1. Bentson, R., S. Nazarian, and J. Harrison, "Reliability Testing of Seven Nondestructive Pavement Testing Devices," a paper prepared with support from the Waterways Experiment Station and the U. S. Department of Transportation and Defense.
2. Hoffmann, M. S., and M. R. Thompson, "Mechanistic Interpretation of Nondestructive Pavement Testing Deflections," Report No. FHWA/IL/UI-190, University of Illinois, Urbana, Illinois, June 1981.
3. Bermister, D. M., "The General Theory of Stresses and Displacements in Layered Systems," *Journal of Applied Physics*, 1945.
4. Hicks, R. G., "Use of Layered Theory in the Design and Evaluation of Pavement Systems," Alaska Department of Transportation and Public Facilities, July 1982.
5. Uddin, W., A. H. Meyer, W. R. Hudson, and K. H. Stokoe, II, "A Methodology for Structural Evaluation of Pavements Based on Dynamic Deflections," Research Report 387-1, Center for Transportation Research, The University of Texas at Austin, July 1985.
6. Bush, A. J., III, "Nondestructive Testing for Light Aircraft Pavements, Phase II, Development of the Nondestructive Evaluation Methodology," Report No. FAA-RD-80-9-11, Geotechnical Laboratory, U.S. Army Engineer Waterways Experiment Station, Vicksburg, Mississippi, 1980.
7. Uzan, J., R. L. Lytton, and F. P. Germann, "General Procedures for Back-Calculating Layer Moduli," First Symposium on NDT of Pavements and Back-calculation of Moduli, American Society for Testing and Materials, Baltimore, Maryland, July 1988.
8. Roesset, J. M., and K. Y. Shao, "Dynamic Interpretation of Dynaflect and Falling Weight Deflectometer Tests," *Transportation Research Record 1022*, Transportation Research Board, National Research Council, Washington, D. C., 1985.
9. Anderson, M., and V. Drenvich, "A True Dynamic Method for Nondestructive Testing of Rigid Pavements with Overlays," *Proceedings*, 4th International Conference on Concrete Pavement Design and Rehabilitation, Purdue University, West Lafayette, Indiana, 1989.
10. Kausel, E., and J. M. Roesset, "Stiffness Matrices for Layered Soils," Vol 71, No. 6, *Bulletin of the Seismological Society of America*, December 1981.
11. Nielson, J. P., "Implications of Using Layered Theory in Pavement Design," *Transportation Engineering Journal*, ASCE, November 1970.
12. Shao, K. Y., J. M. Roesset, and K. H. Stokoe, II, "Dynamic Implementation of Dynaflect and Falling Weight Deflectometer Plots on Pavement Systems," Research Report 437-1, Center for Transportation Research, The University of Texas at Austin, August 1986.
13. Uddin, W., A. H. Meyer, and W. R. Hudson, "Rigid Bottom Considerations for Nondestructive Evaluation of Pavements," *Transportation Research Record 1070*, Transportation Research Board, Washington, D. C., 1987.
14. Briggs, R. C., and S. Nazarian, "Effects of Unknown Rigid Subgrade Layers on Backcalculation of Pavement Moduli and Projection of Pavement Performance," a paper presented at the 1989 Annual Meeting of the Transportation Research Board, Washington, D. C., January 1989.
15. Barber, E. S., "Calculation of Maximum Pavement Temperatures from Weather Reports," Highway Research Bulletin 168, Highway Research Board, Washington, D. C., 1957.
16. Stokoe, K. H., II, S. Heisey, and A. H. Meyer, "Moduli of Pavement Systems from Spectral Analysis of Surface Waves," *Transportation Research Record No. 852*, Washington, D.C., 1982.
17. Nazarian, S., and K. H. Stokoe, II, "Use of Surface Waves in Pavement Evaluation," *Transportation Research Record No. 1070*, Washington, D.C., 1983.
18. Rix, G. J., and K. H. Stokoe, II, "Stiffness Profiling of Pavement Subgrades," *Transportation Research Record*, Washington, D.C., 1989 (in press).
19. Roesset, J. M., P. Chang, K. H. Stokoe, II, and M. Aouad, "Modulus and Thickness of the Pavement Surface Layer from SASW Tests," a paper prepared for publication at the 1990 Annual Meeting of the Transportation Research Board, January 1990.

20. Richart, F. E., Jr., J. R. Hall, Jr., and R. D. Woods, *Vibrations of Soils and Foundations*, Prentice-Hall, Englewood Cliffs, New Jersey, 1970.

21. Stokoe, K. H., II, and R. J. Hoar, "Variables Affecting In Situ Seismic Measurements," *Proceedings*, Conference on Earthquake Engineering and Soil Dynamics, ASCE Geotechnical Engineering Division, Vol II, pp 919-939, 1978.

22. Ni, S. H., and K. H. Stokoe, II, "Evaluation of an Isotropic Shear Modulus with Resonant Column Device," Report GR85-8, Civil Engineering Department, The University of Texas at Austin, 1985.

23. Claros, G., W. R. Hudson, and K. H. Stokoe, II, "Modifications to the Resilient Modulus Testing Procedure and the Use of Synthetic Samples for Equipment Calibration," Transportation Research Board, Washington, D. C., January 1990.

24. Stokoe, K. H., II, and S. H. Ni, "Effects of Stress State and Amplitude on Shear Modulus of Dry Sand," *Proceedings*, Second Symposium on the Interaction of Non-Nuclear Munitions with Structures, p 407, 1985.

25. Seed, H. B., and I. M. Idriss, "Shear Moduli and Dampling Factors for Dynamic Response Analyses," Earthquake Engineering Research Center, University of California at Berkeley, California, Report No. EERC70-10, 1970.

26. Chomton, G., and P. J. Valyer, "Applied Rheology of Asphalt Mixes: Practical Application," *Proceedings*, Third International Conference on Structural Design of Asphalt Pavements, Vol I, University of Michigan, Ann Arbor, 1972.